

University of Groningen

2D and 3D Covalent Organic Frameworks

Yazdani, Hossein; Shahbazi, Mohammad-Ali; Varma, Rajender S.

Published in:
ACS Applied Bio Materials

DOI:
[10.1021/acsabm.1c01015](https://doi.org/10.1021/acsabm.1c01015)

IMPORTANT NOTE: You are advised to consult the publisher's version (publisher's PDF) if you wish to cite from it. Please check the document version below.

Document Version
Publisher's PDF, also known as Version of record

Publication date:
2022

[Link to publication in University of Groningen/UMCG research database](#)

Citation for published version (APA):

Yazdani, H., Shahbazi, M-A., & Varma, R. S. (2022). 2D and 3D Covalent Organic Frameworks: Cutting-Edge Applications in Biomedical Sciences. *ACS Applied Bio Materials*, 5(1), 40–58.
<https://doi.org/10.1021/acsabm.1c01015>

Copyright

Other than for strictly personal use, it is not permitted to download or to forward/distribute the text or part of it without the consent of the author(s) and/or copyright holder(s), unless the work is under an open content license (like Creative Commons).

The publication may also be distributed here under the terms of Article 25fa of the Dutch Copyright Act, indicated by the "Taverne" license. More information can be found on the University of Groningen website: <https://www.rug.nl/library/open-access/self-archiving-pure/taverne-amendment>.

Take-down policy

If you believe that this document breaches copyright please contact us providing details, and we will remove access to the work immediately and investigate your claim.

Downloaded from the University of Groningen/UMCG research database (Pure): <http://www.rug.nl/research/portal>. For technical reasons the number of authors shown on this cover page is limited to 10 maximum.

2D and 3D Covalent Organic Frameworks: Cutting-Edge Applications in Biomedical Sciences

Hossein Yazdani,* Mohammad-Ali Shahbazi, and Rajender S. Varma*

Cite This: *ACS Appl. Bio Mater.* 2022, 5, 40–58

Read Online

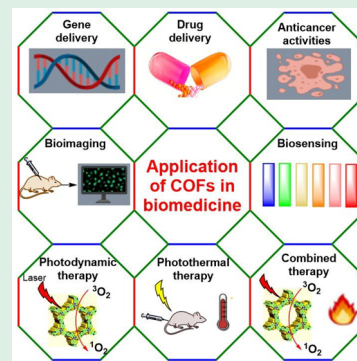
ACCESS |

Metrics & More

Article Recommendations

ABSTRACT: Covalent organic frameworks (COFs) are crystalline porous organic structures with two- or three-dimensional (2D or 3D) features and composed of building blocks being connected via covalent bonds. The manifold applications of COFs in optoelectronic devices, energy conversion and storage, adsorption, separation, sensing, organocatalysis, photocatalysis, electrocatalytic reactions, and biomedicine are increasing because of their notable intrinsic features such as large surface area, porosity, designable structure, low density, crystallinity, biocompatibility, and high chemical stability. These properties have rendered 2D and 3D COF-based materials as desirable entities for drug delivery, gene delivery, photothermal therapy, photodynamic therapy, combination therapy, biosensing, bioimaging, and anticancer activities. Herein, different reactions and methods for the synthesis of 2D and 3D COFs are reviewed with special emphasis on the construction and state-of-the-art progress pertaining to the biomedical applications of 2D and 3D COFs of varying shapes, sizes, and structures. Specifically, stimuli-responsive COFs-based systems and targeted drug delivery approaches are summarized.

KEYWORDS: COFs, porous materials, biomedical application, drug delivery, gene delivery, biosensing, photodynamic therapy



1. INTRODUCTION

Covalent organic frameworks (COFs) make up a class of porous organic structures with tunable pore size, high crystallinity, unique molecular architecture, and large specific surface area and are constructed by diverse covalent bonds among light elements (e.g., H, B, C, N, and O). These structures were initially introduced by Yaghi and colleagues in 2005¹ and have been prepared in two-dimensional (2D-COFs) and three-dimensional forms (3D-COFs) or weaving frameworks (Figure 1).^{1–3} In addition, COF crystallites have been reported in varying shapes such as sheets, fibers, foams, cubes, belts, platelets, spheres, and rectangular prisms.^{4–8}

Several reactions have been deployed for the construction of COFs including Schiff base condensation,⁹ hydrazine¹⁰ and imide formation,² Knoevenagel condensation,¹¹ amide bond formation via the reaction between amine and acyl chloride,¹² phenazine formation,¹³ aromatic nucleophilic substitution,¹⁴ and the formation of spirobrute,¹⁵ benzoxazole,¹⁶ benzothiazole,¹⁷ and benzimidazole,¹⁸ multicomponent reaction based on the Strecker reaction,¹⁹ three-component one-pot Povarov reactions,¹⁹ three-component reactions for the construction of imidazole via Debus-Radziszewski reaction,²⁰ Michael addition reaction,²¹ amination formation,²² self-condensed of boronic acids to six-membered boroxine,¹ co-condensation of boronic acids with dialcohols to five-membered boronate ester,^{1,23} trimerization of nitriles to triazine,²⁴ dimerization of nitroso,²⁵ and trimerization of borazine.²⁶

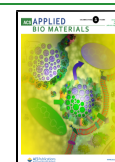
As the preparative strategies pertaining to assembly of COFs have been summarized in some literature reviews,^{27–30} the syntheses of COFs are just briefly mentioned further (Figure 2):

- (1) Solvothermal synthesis: It was the first approach for the synthesis of COFs disclosed in 2005 by Yaghi and co-workers, and most of the COFs have been synthesized via this protocol. The synthesis is often carried out in glovebox at distinct pressure (150 Torr being optimal pressure in the vacuum line) and heating about 80–120 °C for 2 to 9 days. The temperature, pressure, and reaction time have been important parameters in this synthesis method.¹
- (2) Microwave (MW) approach was developed for the COFs synthesis by Cooper and co-workers in 2009. The main advantages of this strategy include more expeditious reaction (60 min) than solvothermal synthesis (72 h) and no need for a sealed system (airtight container).^{31,32}
- (3) Ionothermal synthesis was introduced by Thomas and colleagues for the synthesis of COFs in 2008, which requires a pyrex tube and high temperatures (about 400

Received: September 20, 2021

Accepted: December 1, 2021

Published: December 14, 2021



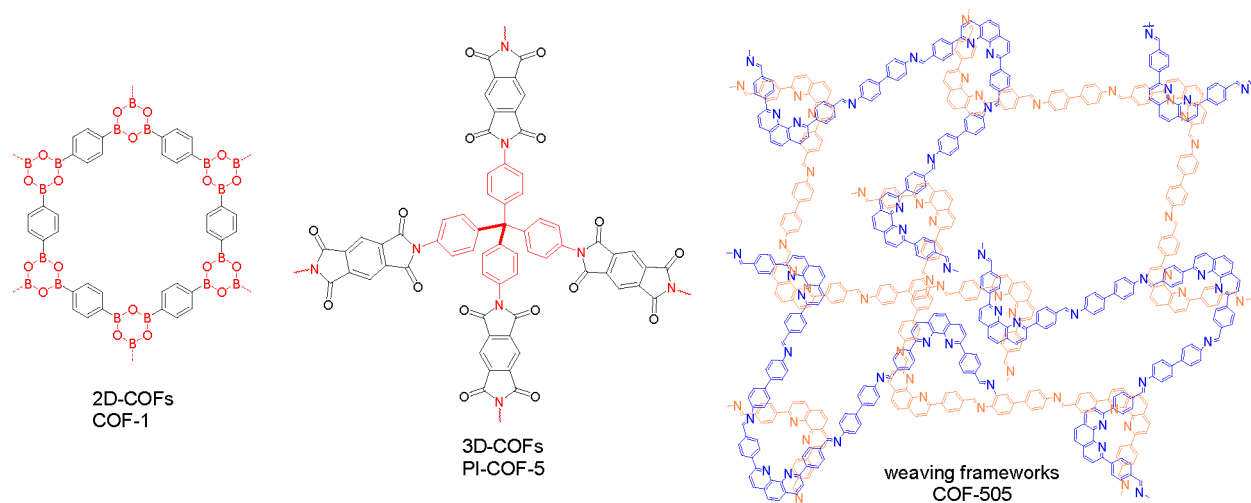


Figure 1. Examples of 2D-COFs, 3D-COFs, and weaving frameworks.

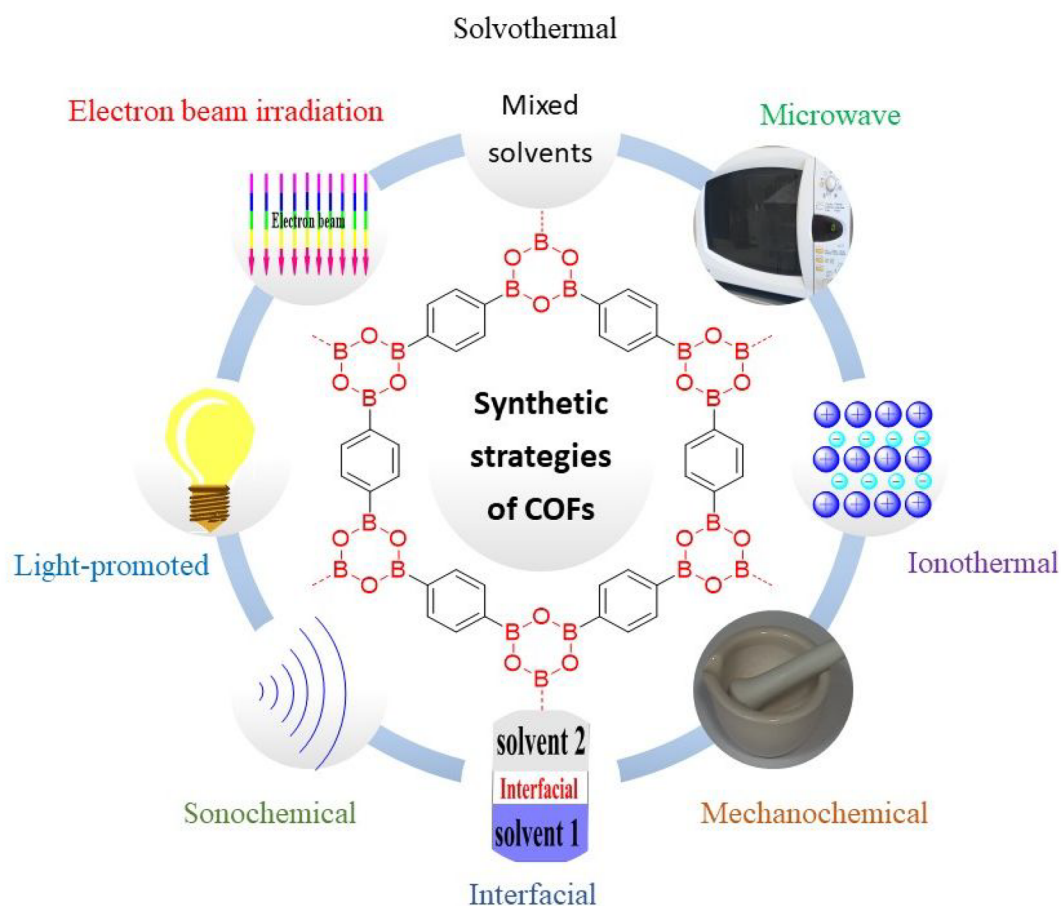


Figure 2. Various synthesis strategies available for the formation of 2D and 3D COFs including solvothermal synthesis, MW approach, ionothermal, MC, interfacial, sonochemical, light-promoted synthesis, and electron beam irradiation approach.

°C) for a long time (2 days). In this strategy, the reaction is carried out in the presence of ionic liquid or molten salt, which serves a dual function as both a catalyst and a solvent.³³

(4) Mechanochemical (MC) synthesis was introduced in 2013 by Banerjee and co-workers to produce crystalline porous COFs as a simple, fast, solvent-free, inexpensive, and scalable method that could be performed at room temperature by means of simple grinding in a mortar and

pestle, enabling the switch from the use of solvents to the solid-state synthesis of COFs. One of the disadvantages of the MC strategy is poor porosity and low crystallinity of the produced COFs in comparison to the solvothermal analogs.³⁴

(5) Interfacial synthesis has been a well-adapted protocol for the construction of polymer thin films in a bulk scale. This efficient strategy has been applied for the synthesis of COFs thin films with control of a tunable thickness. In this

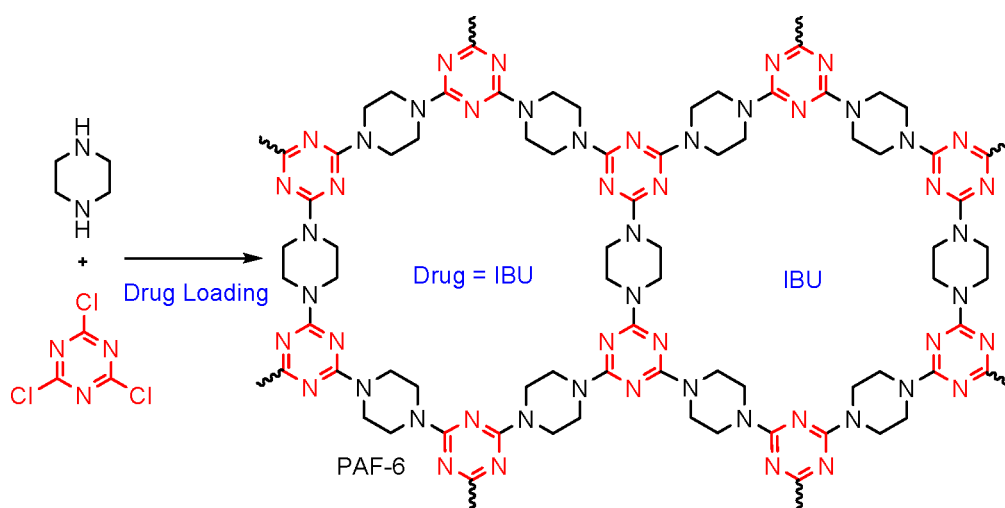


Figure 3. Schematic for the synthesis of PAF-6 as a 2D triazine-piperazine-based framework for IBU delivery.

regard, solid–liquid interface reactions, air/water interface, liquid/liquid interface, and a liquid/liquid/gel triphase system are various types of systems that can be used depending on the phases involved.³⁵

- (6) Sonochemical synthesis is another route wherein an effective mixing via a cavitation phenomenon proceeds in a short reaction time and without bulk high temperatures and high pressures. The key part of sonochemistry is the formation, growth, and collapse of bubbles that this process is called acoustic cavitation.³⁶
- (7) Light-promoted synthesis enables the fabrication of COFs utilizing abundant light (for example, simulated sunlight irradiation at wavelength 200–2500 nm) as an energy source. Improved crystallinity is one of the advantages of this strategy.³⁷
- (8) Electron beam irradiation (1.5 MeV) at room temperature accomplishes the preparation within minutes, which is amendable for large-scale production of COFs.³⁸

Over the past few years, COFs have attained the status of a propitious platform with fascinating properties such as large surface areas, superb visible light absorbance, tunable band gaps, and long-range order structures that have displayed outstanding performance in diverse applications. They include appliances in optoelectronic device, membranes,^{39,40} gas separation and storage (e.g., ammonia uptake, capture of CO₂, SO₂ and NO, separation of hydrogen isotopes, purification of H₂ and CH₄, and separation of acetylene from ethylene), sensing, optical thermometer, organocatalysis, photocatalysis (H₂ evolution, photoredox organic transformations), energy conversion and storage, light emitters, catalysis (C–C coupling reactions, oxidations, reductions, asymmetric synthesis, Heck-epoxidation tandem reaction, chemical fixation of CO₂, cycloaddition, and condensation), electrocatalytic reactions (electrochemical CO₂ reduction, oxygen reduction reactions (ORR), and oxygen evolution reactions (OER)), and separation (dye separation, removal of organic contaminants from water, seawater desalination, removal of toxic ions, extraction of thorium from uranium and chiral separation);^{27,28,40,41} in addition, π conjugation, low density, high stability to hydrolysis in reductive and oxidative environments, tunable porosity, large surface area and biocompatible properties of COFs have enabled them to serve as an extremely favorable platform in biomedical fields, including drug delivery, photodynamic therapy, photothermal

therapy, and combined therapy, bioimaging, biosensing, and anticancer activities, among others.

COFs have garnered widespread attention since their discovery, and review articles have focused on chemistry beyond the structure, topology, shape, construction, and application in separation, sensing, organic chemistry, catalysis, electrocatalysis, and photocatalysis.^{27,28,40,42} However, there are only a few reviews that have exclusively discussed the appliances of COFs in the biomedical arena.^{43–47}

Herein, particular emphasis has been on the fabrication and application of 2D and 3D COFs as a platform, which can be exploited as a promising nanopatform for biomedical application and practical clinical trials. In the present review article, stimuli-responsive COFs-based systems and targeted drug delivery are summarized for *in vitro* and *in vivo* investigations. Photodynamic-, photothermal-, and combination therapy are appraised. Finally, some selected examples for biosensing and bioimaging application of COFs are discussed.

2. COFS: CUTTING-EDGE APPLICATION IN DRUG DELIVERY

Nontarget accumulation and multidrug resistance are two main limitations for the effective delivery of drugs to cells and tissues.⁴⁸ For surmounting these limitations, a tremendous global effort has been devoted to the development of drug-loaded carriers for efficient and nontoxic drug delivery systems.^{49–52} Many studies have investigated the use of COFs in drug delivery; 2D porous organic frameworks (POFs) for drug delivery have been reported in 2011.⁵³ Through nucleophilic substitution reaction, the linear linking unit, piperazine, reacts with the cyanuric chloride as a trigonal building unit to generate 2D POFs, named PAF-6 (Figure 3). *In vitro* testing of the pure framework revealed almost no cytotoxicity over the range of concentrations tested in cell viability assays with HeLa cells, confirming that PAF-6 is a nontoxic and biocompatible architecture deployable in biomedical applications. Then ibuprofen (IBU), an anti-inflammatory drug that is widely used for the treatment of pain, inflammation, and rheumatism, was loaded in PAF-6. *In vitro* release in PBS at pH 7.4 displayed that 50% of the drug was released within 5 h, and 75% within 10 h, and it took about 46 h to have all the drug released from the framework.⁵³ Compared with MOFs, such as MIL-101⁵⁴ and MIL-53,⁵⁵ that have been

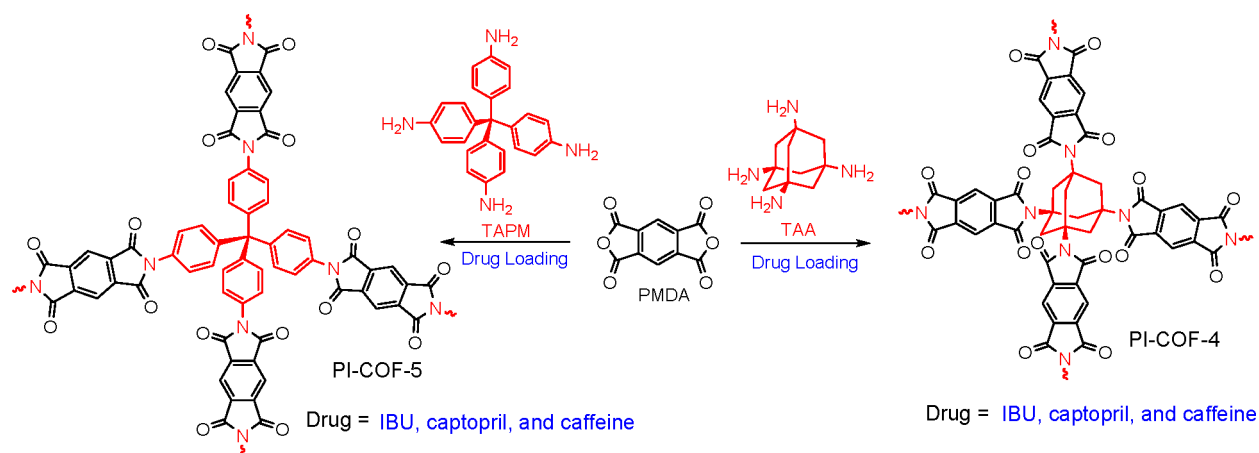


Figure 4. Construction of 3D PI-COF-4 and PI-COF-5 and their application as carriers for IBU, caffeine, and captopril.

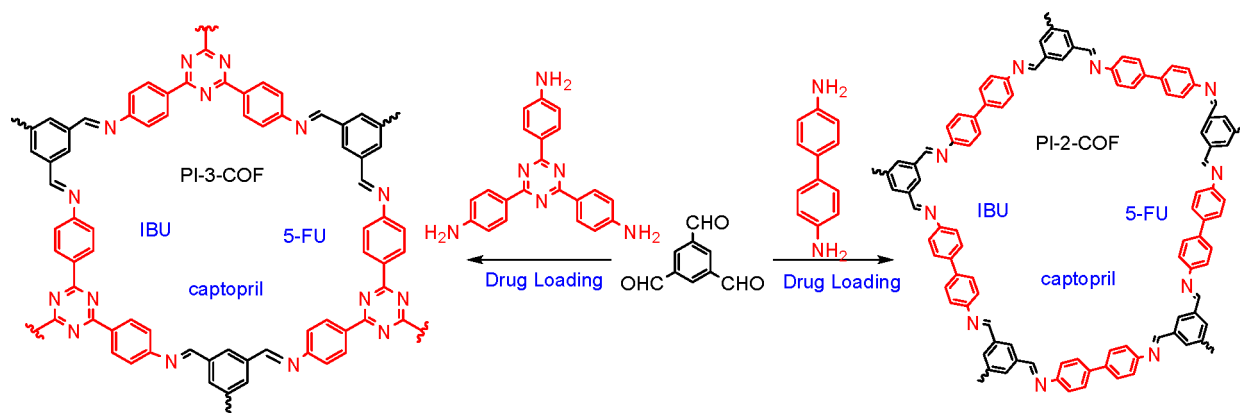


Figure 5. 2D PI-3-COF and 2D PI-2-COF for loading of IBU, 5-FU, and captopril.

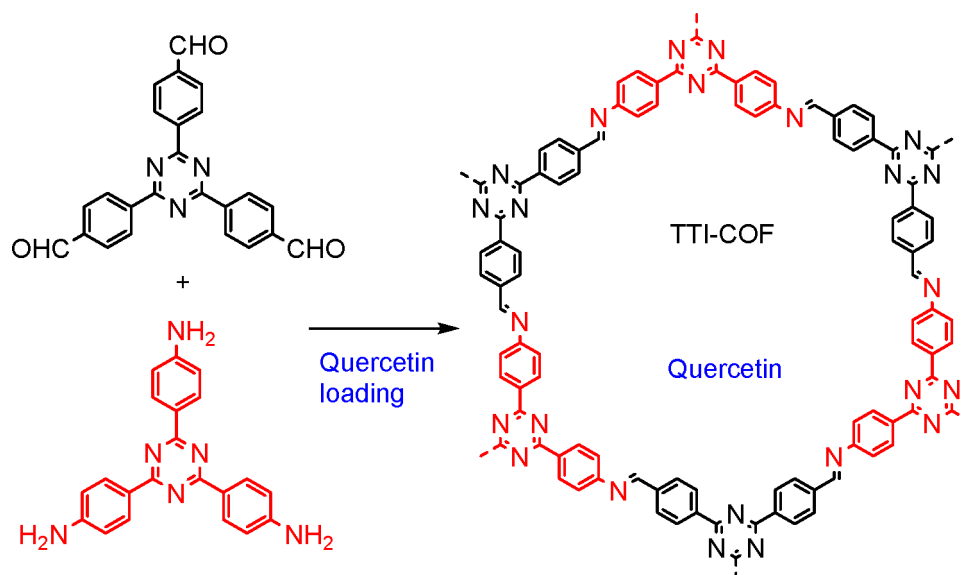


Figure 6. Fabrication of TTI-COF-based quercetin delivery nanomaterials.

scrutinized for drug delivery, the PAF-6 showed a high release rate, thus exemplifying an unprecedented use of POFs in drug delivery. In 2015, two 3D porous crystalline polyimides (PI-COFs) were synthesized by Yan and co-workers;² 3D porous PI-COF-4 and PI-COF-5 were prepared via the imidization reaction of pyromellitic dianhydride (PMDA) with 1,3,5,7-

tetraaminoadamantane (TAA) or tetra(4-aminophenyl)methane (TAPM) (Figure 4). On the basis of the sizes of TAA and TAPM (3.1 and 5.9 Å) and their formative bisimide links (13.0 and 18.6 Å), noninterpenetrated (PI-COF-4) or 4-fold-interpenetrated (PI-COF-5) diamond nets could be achieved by dehydration of the dianhydride to produce linear



Figure 7. Schematic representation of TpASH-FA CONs for targeted drug delivery. Reprinted with permission from ref 58. Copyright 2017 American Chemical Society.

bisimides. The pore sizes of the PI-COF-4 and PI-COF-5 were 13 and 10 Å, respectively, which were calculated by nonlocal density functional theory. The molecular size of IBU is 5 Å × 10 Å, which could be entrapped by PI-COFs. IBU was loaded in both PI-COF-4 and PI-COF-5 with concentrations of 24 and 20 wt %, respectively, based on TGA data. The release profile of IBU-loaded 3D PI-COFs was evaluated, showing 60% of drug release for PI-COF-4 and 49% for PI-COF-5 after 12 h, respectively, while all IBU was released after 6 days for both the PI-COFs. Compared to PAF-6, both 3D PI-COFs displayed a lower release rate. Likewise, PI-COF-5 with a smaller pore size and 4-fold-interpenetrated architecture exhibited a lower release rate than PI-COF-4 with a bigger pore size and non-interpenetrated structure. This observation affirmed that the drug release from COFs is dependent on the geometry and pore size. Further investigations of PI-COF-4 and PI-COF-5 for drug delivery applications included caffeine as a psychoactive drug and captopril as antihypertension, wherein a high loading and good release were revealed for both 3D PI-COFs.²

In another study, two imine-based 2D COFs, PI-3-COF and PI-2-COF, were fabricated under solvothermal conditions via the condensation between 1,3,5-triformylbenzene and 2,4,6-tris(4-aminophenyl)-s-triazine or 4,4'-biphenyldiamine, respectively (Figure 5). The pore sizes of these 2D COFs were 11 Å for PI-3-COF and 14 Å for PI-2-COF as determined by Brunauer–Emmett–Teller (BET) analysis. IBU, 5-fluorouracil (5-FU), and captopril were employed for loading and release study where PI-2-COF with a larger pore size displayed higher drug loading capacity, demonstrating that the pore size and geometry of COFs directly affect the capability of drug loading. The drug release rate was almost identical for both 5-FU@PI-3-COF and 5-FU@PI-2-COF as the majority of the 5-FU was released after ~3 days, and the total delivery amount could reach up to 85% of the initial 5-FU loading. *In vitro* studies of the pure frameworks displayed good biocompatibility and low cytotoxicity with two other drugs, IBU and captopril, revealing the same release profile as 5-FU.⁵⁶

The delivery of quercetin (3,3',4',5,7-pentahydroxyflavone) deploying COFs as nanocarrier was reported as a hydrophobic drug with poor solubility and low bioavailability. The reaction between the triazine triphenyl aldehyde (TT-ald) and triazine triphenylamine (TT-am) was conducted to form triazine triphenyl imine-COF (TTI-COF) (Figure 6), which was used for the transport of quercetin into TTI-COF via π - π interactions and hydrogen-bond interactions between imine nitrogen in COF and hydroxyl groups in quercetin molecule as confirmed by solid-state NMR studies. The quercetin-loaded framework caused the apoptosis of human breast carcinoma MDA-MB-231 cells.⁵⁷ However, TTI-COF has some drawbacks such as the lack of targeting groups. To solve this issue, COFs, namely, TpASH (Tp, 1,3,5-triformylphloroglucinol; ASH, 4-aminosalicylhydrazide), were prepared via solid-state mixing strategy followed by three postsynthetic modifications to afford covalent organic nanosheets (CONs) (TpASH-FA; FA, folic acid) as a targeting carrier for cancer therapy by encapsulating 5-FU (Figure 7). The results showed sustained release of 5-FU within the breast cancer cells MDA-MB-231, through receptor-mediated endocytosis, which led to the apoptosis of cancer cells, although TpASH-FA had some limitations such as a lack of *in vivo* studies and biodegradation kinetics.⁵⁸

In vivo studies are absolutely crucial for the practical clinical applications, and the design of excellent and efficient cargos for this purpose requires several desirable factors including (1) good dispersibility in aqueous media and, subsequently, bioaccessibility to cells, (2) suitable particle size (the optimal size for cellular uptake should be below 200 nm), and (3) *in vivo* cytotoxicity must be minimal, and cargos should have good biocompatibility. In this context, water-dispersible polymer-COF nanocomposites as smart carriers for *in vitro* and *in vivo* drug delivery have been reported. A linear tail polymer (denoted as PEG-CCM) was prepared by the combination of polyethylene glycol (PEG) and curcumin (CCM). Amine-functionalized COFs (denoted as APTES-COF-1 or COF-1) were realized via Brønsted-type interactions between amine groups in

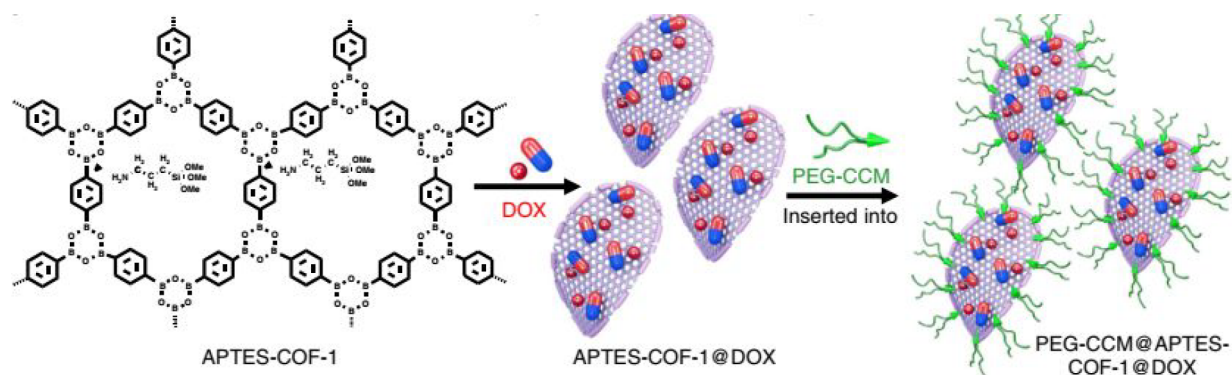


Figure 8. Schematic representation of micelle PEG-CCM@APTES-COF-1@DOX.

(3-aminopropyl)triethoxysilane (APTES) and boron atoms in COFs, and then DOX was loaded into APTES-COF-1, which is named as APTES-COF-1@DOX. DOX bearing aromatic ring and amine and hydroxy groups can be loaded onto the COF via both the hydrogen bonding and π - π interactions. The entire structure of the micelle (PEG-CCM@APTES-COF-1@DOX) was attained by assembling PEG-CCM as the corona and APTES-COF-1@DOX as the core (Figure 8). Compared with bare APTES-COF-1, the PEG-CCM@APTES-COF-1 presented a higher loading efficiency of DOX with a loading capacity of 9.71 ± 0.13 wt % and encapsulation efficiency of $90.5 \pm 4.1\%$. The explanations for these results come from the imparted hydrophilicity of PEG, which improved its stability and dispersion in aqueous media. After intravenous injection, DOX was released via unplugged PEG-CCM, and then the progress of cellular uptake and DOX release was tracked by monitoring the fluorescence of CCM and DOX in a real time manner. *In vivo* studies revealed an enhanced tumor-inhibition effect for the PEG₂₀₀₀-CCM@APTES-COF-1@DOX nanocomposite in tumor-bearing mice when compared with the free DOX formulation, APTES-COF-1@DOX system, and other formulations of PEG_n-CCM@APTES-COF-1@DOX ($n = 350$ and 1000). Besides, PEG₃₅₀-CCM@APTES-COF-1 showed an efficient targeting capability toward brain tumors.⁵⁹

Currently, stimuli-responsive systems and materials are extensively explored for drug delivery.^{60–62} Stimuli-responsiveness can be classified into two groups of internal (temperature, pH, enzyme, glucose, reactive oxygen species (ROS), glutathione (GSH)) and external (light, ultrasound, mechanical, electrical field, and magnetic field).⁴⁹ GSH-responsive nanocarriers based on materials have been evaluated to improve the accumulation and retention of drugs in tumors and other injured cells, which display overexpression of GSH. Intracellular GSH concentration usually ranges from 0.5 to 10 mM⁶³ and is available ~90% in the cytosol, and almost ~10% is in the mitochondria, with a very small percentage being in the endoplasmic reticulum.⁶⁴ GSH plays an important biological role in living organisms and their levels are increased in various types of tumors, which causes the neoplastic tissues more resistant to chemotherapy.⁶⁵ Accordingly, the development of GSH-responsive structures is needed to a greater extent for drug delivery as exemplified by GSH-responsive COFs (denoted as F68@SS-COFs) constructed by self-assembly of polyoxyethylene-polyoxypropylene block copolymer (PEG-PPO-PEG) with disulfide-bearing COFs derivatives prepared via the Schiff base condensation between 4-aminophenyl disulfide (DDS) and benzene-1,3,5-tricarboxaldehyde (BTA).

The drug loading capacity of DOX into the pores of the framework was 21%, which was attributed to the framework pores endowed with π - π stacking interactions. These nanoparticles not only displayed efficient release of DOX to tumor cells but also represented a good response to GSH concentration (10 mM GSH) in tumor cells.⁶⁶ This result suggested that such nanoparticles could be used as promising nanoplatforms for anticancer drug delivery.

The pH-responsive cargos make up a group of materials that can respond to pH changes based on functional groups such as amine and carboxylic groups in their structures.⁶⁷ Recently, pH-responsive COFs have been developed for both *in vitro* and *in vivo* studies. Tri(4-formylphenyl)amines (TPA-CHO) and benzidine reacted via solvothermal strategy to generate pH-responsive COF with intrinsic fluorescent properties (Figure 9).

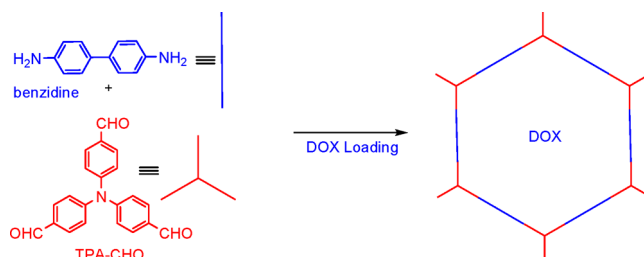


Figure 9. COFs-based DOX delivery nanomaterials.

DOX could be encapsulated with a high loading content of ~35% due to the hydrogen bond and π - π interactions between the drug and COFs. In an acidic environment (e.g., pH = 5.0), with cleavage of interactions between DOX and COFs, the drug could be released and induce a therapeutic effect.⁶⁸

In another study, a pH-responsive COF platform (denoted as TAPB-DMTP-COF) was synthesized via the Schiff base condensation reaction between 2,5-dimethoxyterephthaldehyde (DMTP) and 1,3,5-tris(4-aminophenyl)benzene (TAPB), and DOX was loaded *in situ* into TAPB-DMTP-COF to attain DOX@COF (Figure 10). The amount of DOX in the DOX@COF platform was about 32.1 wt % that displays high drug-loading capacity. At pH 5.0 or 6.5, most of the DOX was released in the first 2 h, and all the drug was released after about 24 h. In contrast, at pH 7.4, about 40% of DOX was released in the first 2 h. The *in vivo* study of pH-responsive DOX@COF has shown its good dispersibility and biocompatibility, low toxicity, and high tumor-suppression efficiency.⁶⁹ Table 1 summarizes the representative COF-based drug delivery systems.

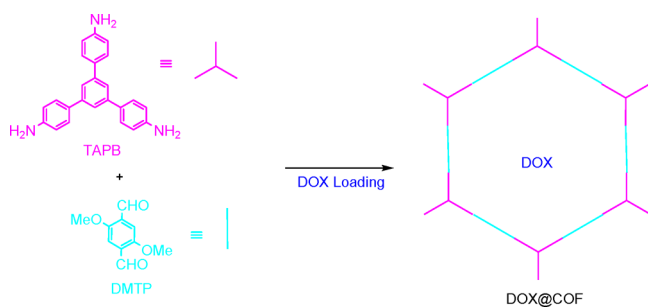


Figure 10. TAPB-DMTP-COF-based DOX delivery nanomaterials.

3. APPLICATION OF COFS IN GENE DELIVERY

Gene therapy is the transfer of foreign genetic material into specific cells of the patient that holds great promise for treating inherited and acquired genetic diseases such as cancer, cystic fibrosis, combined immunodeficiency, and Parkinson's via rectifying the genomic errors.⁷¹ In transfer naked genes such as small interfering RNA (siRNA), mRNA (mRNA), plasmid DNA (pDNA), and antisense oligonucleotides (ASOs) to targeted cells at the targeted site do not achieve desired outcomes due to their rapid enzymatic degradation, low cellular uptake, nonspecific biodistribution, and rapid clearance;⁷² therefore, effective delivery of therapeutic genes to targeted tissues requires a carrier/nucleic acid system, named vectors that are divided into two categories: viral vectors (e.g., retroviruses, adenoviruses, and lentiviruses) and nonviral vectors (e.g., liposomes, polymers, and inorganic materials such as calcium phosphate).⁷³ Over the past two decades, a wide range of nanoparticulate gene delivery systems have been developed.⁷⁴ Improving the speed, cost effectiveness, safety, and efficiency of intracellular delivery methods remains a long-standing challenge.⁷⁵ COFs have some advantages in gene delivery including excellent gene transfection, good biocompatibility, low cytotoxicity, among others. Dual functionalized covalent triazine framework (CTF) nanosheets, named CTF-PEG-PEI (PEI: polyethylenimine) with brush-like hierarchical structures, were

fabricated through exfoliation and surface chemistry modification. *In vitro* gene delivery studies in both the HeLa and 293T cells reveal that CTF-PEG-PEI has lower cytotoxicity and good gene transfection performance compared to PEI. The lack of *in vivo* trial is one of drawbacks of this study.⁷⁶ In another study, a cationic COF nanoparticle with good dispersion and uniform size was prepared through the one-pot method. This COF-based gene vector exhibited good biocompatibility and excellent gene transfection ability both *in vitro* and *in vivo*.⁷⁷

4. APPLICATION OF COFS IN PHOTODYNAMIC THERAPY

Photodynamic therapy (PDT) has been evaluated for cancer therapy as a potential noninvasive therapeutic method with attributes such as simple operation and low side effects.⁷⁸ Photosensitizers (PSs), oxygen, and specific wavelengths of light are three important elements for PDT.⁷⁹ A large number of PSs (Figure 11) exist including porphyrins,⁸⁰ chlorophylls, cyanine derivatives (IR783, cyanine3, cyanine5, indocyanine green, thiocarbocyanine, and oxacarbocyanine),⁸¹ xanthene derivatives (rose Bengal, rhodamine, fluorescein, and eosin),⁸² and derivatives of coumarin,⁸³ squaraine,⁸⁴ oxadiazole (benzoxadiazole and nitrobenzoxadiazole),⁸⁵ anthraquinones,⁸² pyrene (cascade blue),⁸⁶ oxazine (Nile red and Nile blue),⁸⁷ arylmethine (crystal violet and malachite green), acridine (acridine yellow, acridine orange, and proflavin), and boron-dipyrromethene (BODIPY).⁸⁸

Mechanistically, in PDT subsequent to a specific wavelength light irradiation, PS is excited and generates reactive oxygen species (ROS, such as hydrogen peroxide (H_2O_2), singlet oxygen (1O_2), superoxide ($O_2^{\bullet-}$), hypochlorite (ClO^-), peroxy radical (ROO^{\bullet}), and hydroxyl radical (HO^{\bullet}))^{89,90} to cause necrosis or apoptosis in cancer cells.^{91,92}

Among various porous organic frameworks such as COF,⁹³ MOF,⁹⁴ and others deployed for PDT application, COF-based PDT is one of the most significant members developed. Free photosensitizers with the characteristics of aggregation tendency and low water solubility would cause low selectivity and low

Table 1. Summary of Typical COF-Based Drug Delivery

COF	linkage	drug molecules	key characteristics	ref
3D PI-COF-4 and PI-COF-5	imine	IBU, caffeine, and captopril	first 3D COFs for drug delivery 24% loading capacity and 95% drug release with IBU for PI-COF-4 20% loading capacity and 95% drug release with IBU for PI-COF-5	2
2D PI-3-COF and PI-2-COF	imine	IBU, 5-FU, and captopril	30% maximum loading capacity with 5-FU and 85% drug release with 5-FU for both COFs.	56
TTI-COF	imine	Quercetin	enhanced anticancer activity of quercetin loaded TTI-COF compare to free quercetin	57
TpASH-FA	β -ketoenamine	5-FU	targeted drug delivery 12% loading capacity, 50% drug release at pH 7.4 and 75% drug release at pH 5.0	58
PEG-CCM@APTES-COF-1	boroxine	DOX and CCM	first report of <i>in vivo</i> drug delivery of COF-polymer nanocomposites 9.71 \pm 0.13% loading capacity and 90.5 \pm 4.1% encapsulation efficiency	59
TAPB-DMTP-COF	imine	DOX	pH-responsive COFs 32.1% loading capacity	69
F68@SS-COFs	imine	DOX	GSH-responsive COFs 21% loading capacity	66
fluorescent COF	imine	DOX	pH-responsive COFs with intrinsic fluorescent properties monitoring drug loading with the naked eye 35% loading capacity.	68
DT-COF	imine	carboplatin	targeted drug delivery 31.32% loading capacity	70

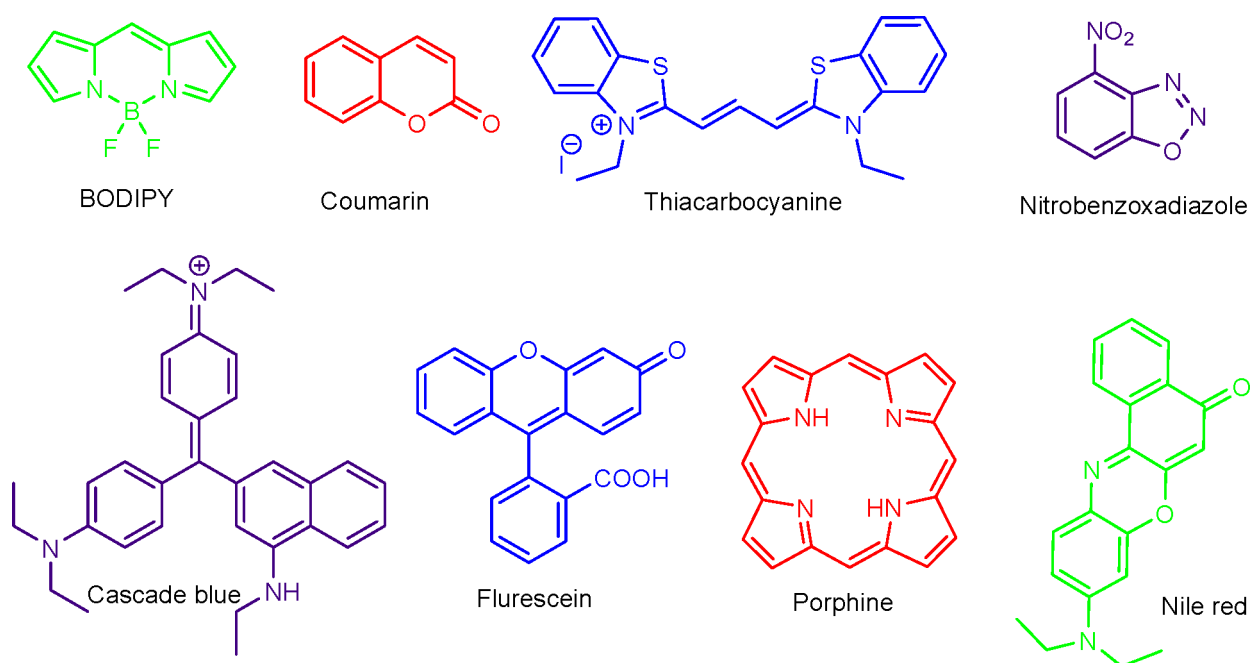


Figure 11. Different types of PSs including BODIPY, coumarin, thiocarbocyanine, nitrobenzoxazole, cascade blue, fluorescein, porphine, and nile red.

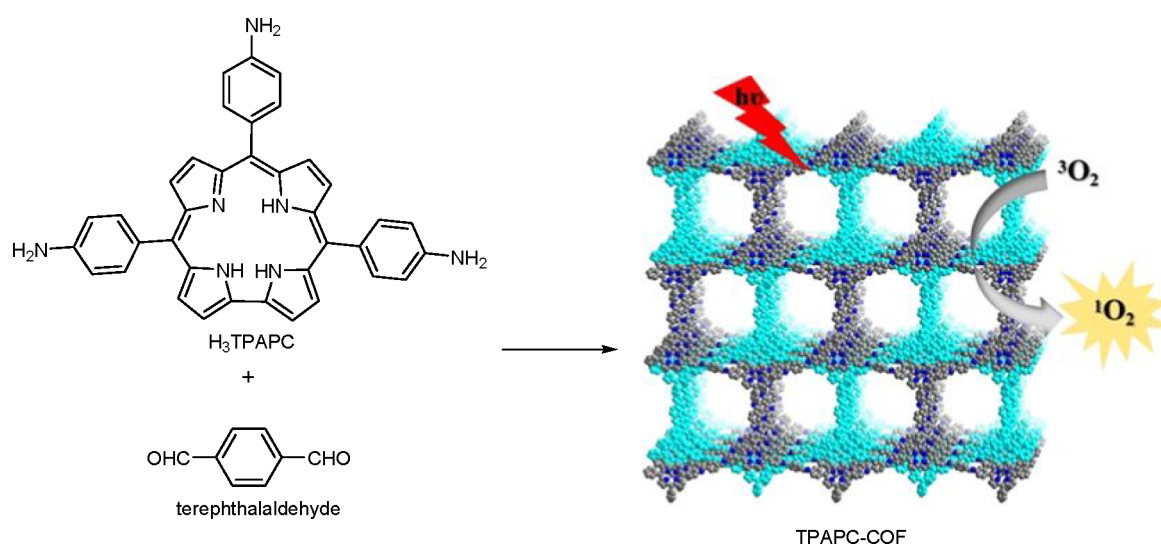


Figure 12. Schematic representation for the synthesis of TPAPC–COF and generating $^1\text{O}_2$. Adapted with permission from ref 102. Copyright 2020 Wiley-VCH.

PDT efficacy toward target tissues, while the COF-based PDT could overcome these drawbacks. 3D Porphyrinic COFs for PDT inactivation of bacteria have been synthesized by Schiff-base reaction between tetrakis(4-aminophenyl)-methane and porphyrinic aldehyde derivatives; under visible light irradiation, they can produce $\text{O}_2(^1\Delta_g)$ that displays strong antibacterial effects toward *Pseudomonas aeruginosa* and *Enterococcus faecalis* biofilms.⁹⁵ In another example, porphyrin-based COF nanodots have been fabricated by the reaction between 5,10,15,20-tetrakis(4-aminophenyl)-21H,23H-porphine (Tph or TAP) and 2,5-dihydroxyterephthalaldehyde (Dha or DHTA) that used a liquid exfoliation method and then modified by PEG. This COF nanodots-PEG system, in the presence of light, produces ROS and shows excellent PDT efficiency in inhibiting tumor growth both *in vitro* and *in vivo* as a result of effective tumor accumulation. The *in vivo* PDT experiments show that

these COF nanodots-PEG can be cleared from the body through renal filtration, rendering them a promising potential for clinical trials.⁹⁶ The real-time and *in situ* monitoring of ROS during PDT in the body is important for minimizing unwanted side effects, evaluating the exact treatment end point, and maximizing the therapeutic effects.^{97,98} The real-time and *in situ* monitoring of ROS generation was performed by upconverting porphyrin-based COF nanoplatfrom (UCCOFs) that have been synthesized using 5,10,15,20-tetrakis(4-aminophenyl)-21H,23H-porphine (TAP), and 2,5 dihydroxyterephthalaldehyde (DHTA). Under NIR irradiation by a 980 nm light, it generated $^1\text{O}_2$ to treat mice bearing 4T1 breast tumors *in vivo* as revealed by an excellent tumor therapeutic effect.⁹⁹

COF_{TTA-DHTA} (TTA: 4,4',4''-(1,3,5-triazine-2,4,6-triyl)-trianiline) has been prepared using solvothermal strategy via

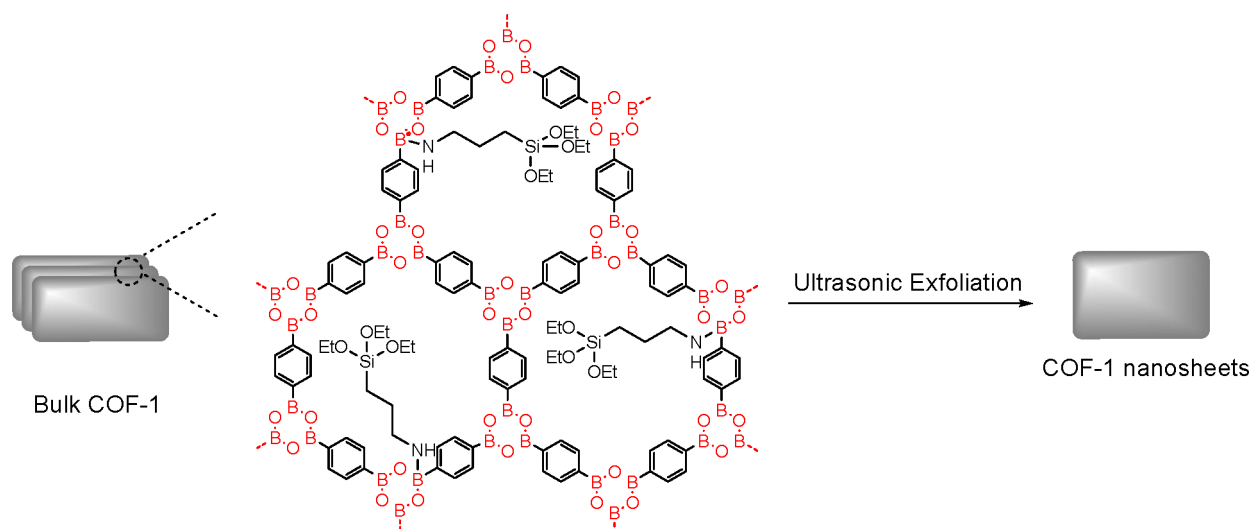


Figure 13. Schematic diagram of PcS@COF-1 nanosheets.

Table 2. Summary of Typical COF-Based PDT, PTT, and Combination Therapy

COF	linkage	application	key characteristics	ref
3D porphyrinic COFs	imine	PDT	displaying strong antibacterial effects toward <i>Pseudomonas aeruginosa</i> and <i>Enterococcus faecalis</i> biofilms	95
porphyrin-based COF nanodots	imine	PDT	showing excellent PDT efficiency in inhibiting tumor growth both <i>in vitro</i> and <i>in vivo</i>	96
UCCOFs	imine	PDT	real-time and <i>in situ</i> monitoring of ROS generation NIR light excitation <i>in vivo</i> study	99
COF _{TTA-DHTA}	imine	PDT	improved ROS generation <i>in vivo</i> study delivery of pirfenidone as an antifibrotic drug	100
COF-909	imine	PDT	Killing over 80% of tumor cells in <i>in vitro</i> studies reduction of tumor size from 9 mm to less than 1 mm in <i>in vivo</i> studies after 10 days treatment	101
TPAPC-COF'	imine	PDT	<i>in vitro</i> assessment of TPAPC-COF' against human breast carcinoma cells corrole-based COF	102
PcS@COF-1	boroxine	PDT	laser irradiation <i>in vitro</i> and <i>in vivo</i> studies displaying photooxidation activity	104
LZU-1-BODIPY	imine	PDT	green LED irradiation (40 mW/cm ²) restraining cancer cells both <i>in vitro</i> and <i>in vivo</i> experiments	105
Fe-HCOF	imine	PTT	laser irradiation showing an excellent antitumor efficacy (87.8%) for the treatment of cancer cells <i>in vivo</i>	107
Fe ₃ O ₄ @COF(TpBD)	imine	PTT	21.5% photothermal conversion efficiency 785 nm light irradiation	108
ICG@COF-1@PDA	boroxine	PDT/PTT	<i>in vitro</i> study against CT26 cells <i>in vivo</i> study against CT26 tumor-bearing mice	112
TP-Por	boronate ester	PDT/PTT	<i>in vitro</i> and <i>in vivo</i> studies	114
COF-LZU-1-CuSe	imine	PDT/PTT	excellent antitumor therapy	115
VONc@TAPB-DMTP-COF-Porph	imine	PDT/PTT	<i>in vitro</i> and <i>in vivo</i> experiments against MCF-7 breast cancer cell 55.9% photothermal conversion efficiency	116
COF@IR783@CAD	boronate ester	chemotherapy/ PTT	excellent <i>in vivo</i> antitumor therapy	118

the condensation between DHTA and TTA. The framework is loaded first with pirfenidone (PFD), an antifibrotic drug, and then is modified with PLGA-PEG (PLGA: poly(lactic-co-glycolic-acid)) to form PFD@COF_{TTA-DHTA}@PLGA-PEG; PLGA-PEG improves the biocompatibility and dispersibility of the nanosystem. After intravenous injection, PFD@COF_{TTA-DHTA}@PLGA-PEG could accumulate and release

PFD in tumor sites, which leads to the downregulation of extracellular matrix components such as collagen I and hyaluronic acid (HA). Followed by injected protoporphyrin IX (PPIX)-conjugated peptide, nanomicelles (NM-PPIX) are formed, which can increase the oxygen supply in the tumor that would be conducive to the improved ROS generation to attain a prominent PDT effect *in vivo*.¹⁰⁰

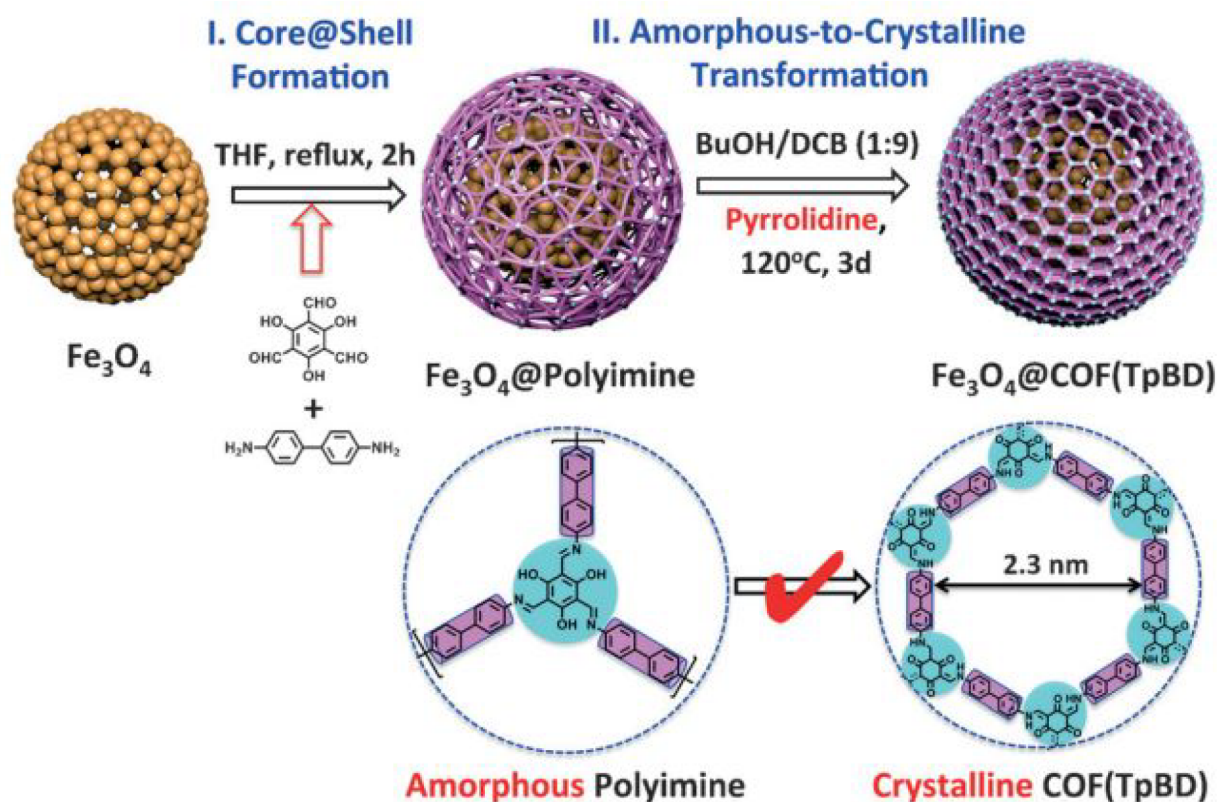


Figure 14. Preparation of $\text{Fe}_3\text{O}_4@\text{COF}(\text{TpBD})$ via the amorphous-to-crystalline conversion process. Reproduced with permission from ref 108. Copyright 2016 Wiley-VCH.

2D COF-909 platform was fabricated by the Schiff base reaction between 4,4',4''-(1,4-phenylene)-bis((2,2':6',2''-terpyridine]-5,5''-dicarbaldehyde)) (L-3N) and *p*-phenylenediamine (PPDA) monomer. Under light irradiation, COF-909 is excited and following by ROS generation in cells to kill over 80% of tumor cells in *in vitro* studies; a 10-day treatment exhibited efficient reduction of tumor size from 9 mm to less than 1 mm *in vivo*.¹⁰¹

In a recent study, 2D corrole-based COF endowed with excellent chemical stability and high crystallinity was synthesized by a reaction between terephthalaldehyde and 5,10,15-tris(*p*-aminophenyl)corrole (H_3TPAPC), labeled as TPAPC-COF (Figure 12). This porphyrin-based COF under 635 nm laser (0.18 W cm^{-2}) irradiation generated $^1\text{O}_2$ (Figure 12). The TPAPC-COF can be further modified with DSPE-PEG2000 as amphiphilic molecules for improving hydrophilicity in the physiological environment (denoted as TPAPC-COF'). *In vitro* assessment of TPAPC-COF' against human breast carcinoma cells not only showed good biocompatibility but also demonstrated the ability to generate the intracellular $^1\text{O}_2$ as a potential PDT application for use in killing cancer cells.¹⁰²

Porphyrin photosensitizer phthalocyanines (PcS) with π -bonds interaction has been incorporated into 2D COF-1 nanosheets.¹⁰³ Then facile ultrasonic exfoliation was performed on these COF nanosheets to achieve nanophotosensitizer based on COF nanosheets, labeled as PcS@COF-1 nanosheets (Figure 13). Under laser irradiation, $^1\text{O}_2$ was generated to restrain the tumor cell proliferation in both *in vitro* and *in vivo* studies. Further, PcS@COF-1 nanosheets displayed photo-oxidation activity by oxidizing dopamine into leucodopamine-chrome.¹⁰⁴

BODIPY-based COF platform has been assembled by the condensation between *tert*-butyl (4-aminophenyl)carbamate (NBPDA) and benzene-1,3,5-tricarbaldehyde under solvothermal conditions. Under green LED irradiation (40 mW/cm^2), $^1\text{O}_2$ was generated to restrain cancer cells both *in vitro* and *in vivo* experiments.¹⁰⁵ Thus, the porous COFs could serve as smart carriers in PDT applications. The representative COF-based PDT systems are summarized in Table 2.

5. APPLICATION OF COFS IN PHOTOTHERMAL THERAPY

Photothermal therapy (PTT) is an emerging photobased treatment that uses electromagnetic radiation such as near-infrared irradiation, visible light, microwaves, and radio-frequency for the treatment of the targeted cells or tissues in which a photosensitive agent is excited with specific band light. This activation brings the sensitizer to an excited state where it releases heat, which kills the targeted cells. Unlike PDT, PTT does not require oxygen to interact with the target abnormal tissues and cells.¹⁰⁶

Presently, new photothermal agents with good biocompatibility, excellent photostability, and efficient photothermal effect are one of the critical issues to achieve minimum side effects and maximum treatment efficacy; COFs have been used for photothermal ablation of cancer cells. Hierarchical COF (HCOF) spheres have been synthesized via a template-free solution-based aging method at room temperature, followed by postsynthetic metalation of HCOF with Fe^{3+} on HCOF. Under laser irradiation, Fe-HCOF exhibited a good photothermal effect and an excellent antitumor efficacy (87.8%) for the treatment of cancer cells *in vivo*.¹⁰⁷

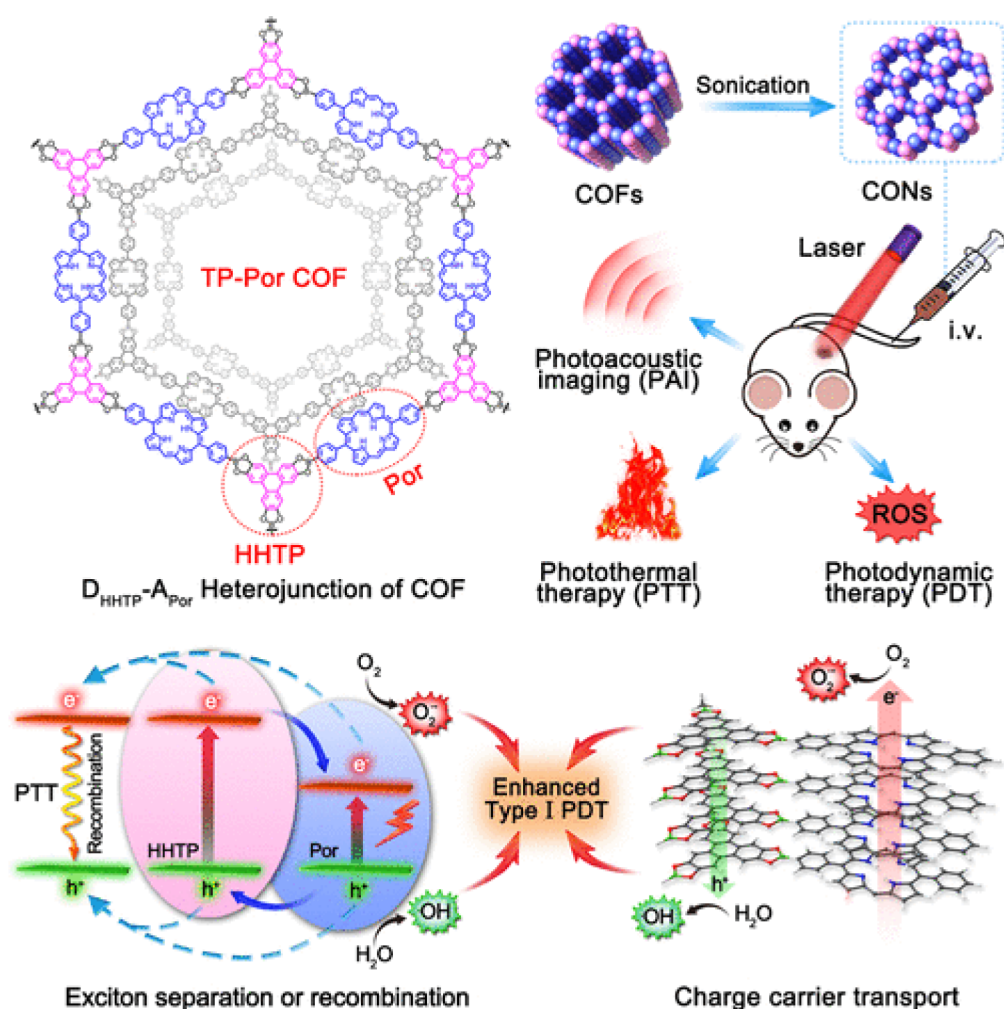


Figure 15. Schematic illustration showing CON construction, the mechanism of PDT and PTT generation, and *in vivo* tumor therapy. Reprinted with permission from ref 114. Copyright 2019 American Chemical Society.

A nano COF layer (denoted as Fe₃O₄@COF(TpBD), BD: benzidine) comprising core–shell nanostructure was used for PTT upon 785 nm light irradiation, with a good photothermal conversion efficiency of 21.5%. The preparation of Fe₃O₄@COF(TpBD) entailed securing a core–shell system consisting of a Fe₃O₄ nanocluster (core) and an amorphous polyimine network (shell). Then the reformation of the polyimine network into the imine linkage COF led to crystalline imine-linked COFs (shell) under solvothermal conditions (Figure 14).¹⁰⁸

Recently, a COF (termed CPF-Cu) was built through the reaction between 2,3-dicyanohydroquinone (DCH) and 1,2,4,5-tetracyanobenzene (TCNB) with Cu riveted in the center as the structure-directing agent. The CPF-Cu exhibited fluorescence quantum yield (10.3%) by UV light and high photothermal conversion efficiency (39.3%) under exposure to near-infrared light;¹⁰⁹ representative COF-based PTT systems are summarized in Table 2.

6. APPLICATION OF COFS IN COMBINATION THERAPY

In the last couple of years, combined therapy, such as the combination of PDT/PTT, and the combination of chemotherapy/PTT, etc., has been gaining ever more attention;^{110,111} the strategy of “killing three birds with one stone” was successfully developed in combination therapy. A combination

therapy comprising PDT and PTT can attain significant antitumor effects. NIR dye indocyanine green (ICG), which forms π – π interaction, was added to COF-1, which is named COF@IR783. Then the ICG@COF-1@PDA nanosystem was prepared by mixing polydopamine (PDA) and COF@IR783 under aqueous sonication exfoliation. Compared with free ICG and COF-1@PDA, ICG@COF-1@PDA displayed stronger photocytotoxicity *in vitro*. Upon NIR laser irradiation, ICG@COF-1@PDA effectively killed CT26 cells by PDT/PTT dual-mode phototherapy. *In vivo* study indicated that the ICG@COF-1@PDA induced by PDT/PTT dual-mode displayed the greatest therapeutic efficacy without notable body weight change against CT26 tumor-bearing mice and potential immune activation against recurrence and metastases.¹¹²

The 2D COF (denoted as TP-Por) has been constructed via a condensation between 5,15-bis(4-boronophenyl)-porphyrin (Por) and 2,3,6,7,10,11-hexahydroxytriphenylene (HHTP) according to the solvothermal strategy.¹¹³ Then CONs were achieved from their bulk COFs via aqueous sonication exfoliation (Figure 15). During the *in vitro* and *in vivo* experiments, the CONs under single-wavelength irradiation exhibited excellent dual-modal properties with significant ROS production (in PDT) and temperature elevation (in PTT). Intravenous injection of CONs in nude mice, followed by the

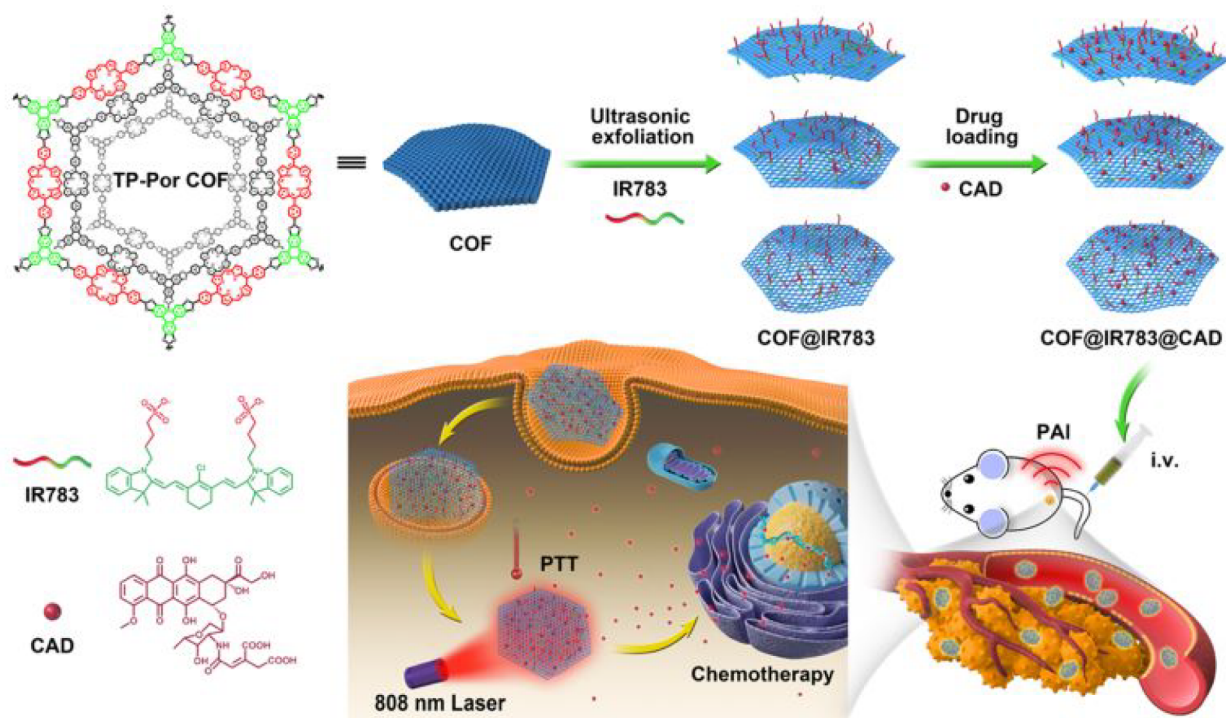


Figure 16. Schematic illustration for construction of COF@IR783@CAD and *in vivo* combinative antitumor therapy. Reprinted with permission from ref 118. Copyright 2019 American Chemical Society.

PDT/PTT, could cause significant tumor ablation without *in vivo* toxicity after 22 days (Figure 15).¹¹⁴

COF-LZU-1 has been generated from 1,3,5-triformylbenzene and 1,4-diaminobenzene according to a facile solution-phase synthesis method at room temperature. Then the COF-LZU-1-CuSe nanocomposites were prepared by the *in situ* conjugation of CuSe nanoparticles with COF-LZU-1. The *in vitro* and *in vivo* experiments demonstrated enhanced tumor suppression efficiency and excellent antitumor therapy of the COF-LZU-1-CuSe platform via a PDT/PTT effect.¹¹⁵

In another report, TAPB-DMTP-COF was fabricated from TAPB and DMTP, while TAPB-DMTP-COF-Porph (Porph: 5-(4-aminophenyl)-10,15,20-triphenylporphyrin) was obtained via Schiff-base condensation between Porph and TAPB-DMTP-COF. Finally, the host-guest supramolecular system VONc@TAPB-DMTP-COF-Porph (VONs: vanadyl 2,11,20,29-tetra(tert-butyl)-2,3-naphthalocyanine) is attained by soaking TAPB-DMTP-COF-Porph in an *N,N*-dimethylacetamide (DMAC) solution of VONc. The ensuing VONc@TPB-DMTP-COF-Porph exhibited an excellent combined PDT/PTT therapeutic effect under the red LED (50 mW/cm²); 808 nm laser irradiation resulted in high ¹O₂ generation with high photothermal conversion efficiency (55.9%). The *in vitro* and *in vivo* experiments unveiled inhibition of MCF-7 breast cancer cell proliferation and metastasis.¹¹⁶

COF-366 has been obtained by the reaction between tetra (*p*-amino-phenyl) porphyrin (TAPP) and terephthaldehyde, which was then converted to nanoparticle form, COF-366 NPs, by ultrasonic dispersion. The COF-366 NPs, upon a single wavelength light, provided an excellent combined PDT/PTT therapeutic effect on 4T1 tumor-bearing mice, which is evidenced by *in vitro* and *in vivo* experiments.¹¹⁷

The condensation reaction between 5,15-bis(4-boronophenyl)-porphyrin and 2,3,6,7,10,11-hexahydroxytriphenylene

(HHTP) afforded a 2D COFs, which were converted to the nanocomposites COF@IR783 via the combination of COFs and IR783 under aqueous sonication exfoliation (Figure 16). Anticancer cisaconityl-doxorubicin (CAD) prodrug was loaded, and combination chemotherapy/PTT with the COF@IR783@CAD was performed in both *in vitro* and *in vivo*; excellent *in vivo* antitumor therapy was realized without *in vivo* toxicity for COF@IR783@CAD (Figure 16).¹¹⁸ The representative COF-based combination therapy systems are summarized in Table 2.

7. APPLICATION OF COFS IN BIOIMAGING

Bioimaging is the observation of entire cells over tissues in whole multicellular organisms and subcellular structures, which uses fluorescence, magnetic resonance, light, electrons, X-ray, and ultrasound as sources for imaging.^{119,120} A bulk material and luminescent triazine-based COF has been prepared by the imine condensation between TTA with 2,6-diformylpyridine (DFP) under 30 min of microwave irradiation to afford the product assigned as TTA-DFP COF. Subsequently, TTA-DFP covalent organic nanosheets (denoted as TTA-DFP CONs), on the nanoscale, were obtained via the exfoliation of the TTA-DFP COF that displayed a high luminescence efficiency with a maximum peak centered at 435 nm. The *in vitro* study revealed that the TTA-DFP CONs exhibited an ability to stain HeLa cell nuclei with no cytotoxic.¹²¹ Still, *in vivo* toxicity evaluation for proper clinical applications of the COFs in bioimaging is a key issue that needs to be addressed in future studies.

A two-photon fluorescent COF nanoprobe, namely, TpASH-NPHS (NPHS: 4-amino-1,8-naphthalimide), was prepared to detect and image intracellular hydrogen sulfide (H₂S) in deep tissues and live cells under NIR excitation, which exhibited high photostability and long-term bioimaging capability.¹²²

Zhang and colleagues reported a benzothiazole-based COF as enhanced fluorescent material for two-photon induced

Table 3. Summary of Typical COF-Based Bioimaging and Biosensing Systems

COF	linkage	application	key characteristics	ref
TTA–DFP CONs	imine	bioimaging	showing a high luminescence efficiency with a maximum peak centered at 435 nm <i>in vitro</i> study against HeLa cell nuclei with no cytotoxic	121
TpASH-NPHS	imine	bioimaging	detect and image intracellular H ₂ S in deep tissues and live cells	122
TPI-COF	imine	bioimaging	two-photon induced fluorescence imaging <i>in vitro</i> and <i>in vivo</i>	123
MCNC@COF@GSH	imine	biosensing	showing excellent performance for endogenous <i>N</i> -linked glycopeptide enrichment in human saliva	125
COF-300-AR	imine	biosensing	detection of GSH levels in HL-60 cells good reusability, light-control, high stability, and catalytic oxidation capacity	126
Ab2/MB/Au@Fe ₃ O ₄ @COF	imine	biosensing	showing linearity ranging from 0.0001–10 ng mL ⁻¹ 30 fg mL ⁻¹ detection limit prostate specific antigen detection	127
TpTTA-COF	imine	biosensing	sensing of adenosine 5'-triphosphate and DNA	128
TPA-COF	imine	biosensing	detection of DNA with high selectivity and excellent sensitivity	129

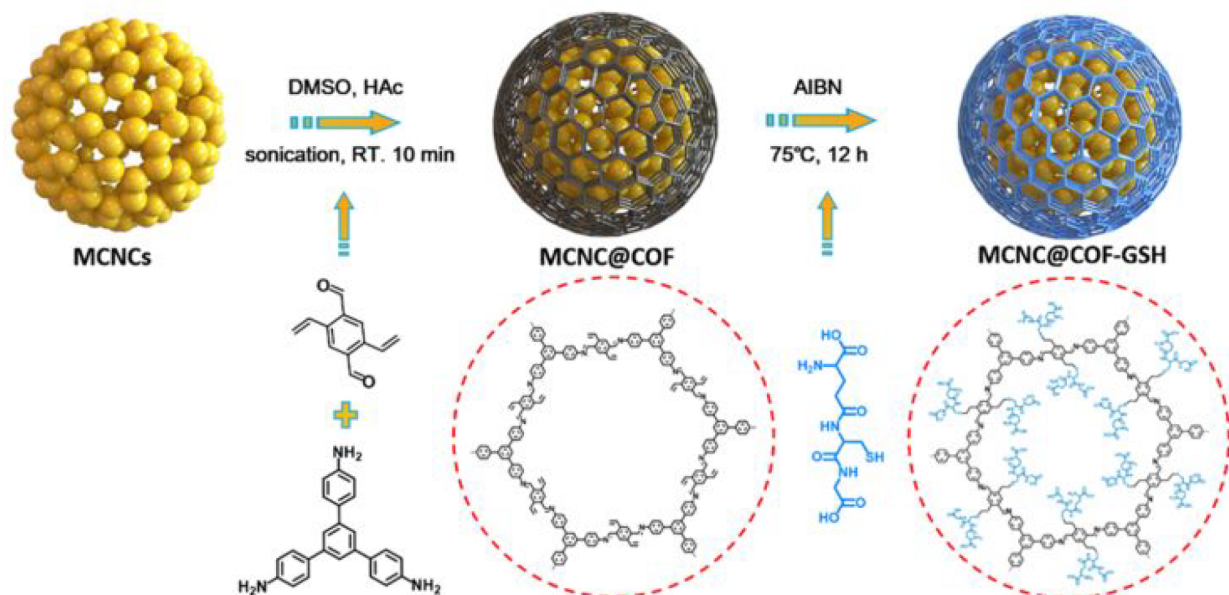


Figure 17. Schematic representation for the synthesis of MCNC@COF@GSH microspheres. Reprinted with permission from ref 125. Copyright 2019 American Chemical Society.

fluorescence imaging *in vitro* and *in vivo*. These TPI-COF (TPI: two-photon induction) were generated via Schiff-base condensation between an aniline building block with a benzothiadiazole-based aldehyde chromophore under solvothermal synthesis protocol.¹²³ The representative COF-based bioimaging systems are summarized in Table 3.

8. APPLICATION OF COFS IN BIOSENSING

Over the past decade, COFs have been extensively utilized for sensing including biosensing, photoelectrochemical-, electrochemical-, QCM-, colorimetric-, humidity-, enantioselective-, and fluorescent sensing.¹²⁴

GSH functionalized magnetic COFs have been synthesized through postsynthetic modification of a vinyl-functionalized magnetic COF for efficient *N*-linked glycopeptide enrichment. The core-shell-structured magnetic COFs were fabricated using magnetic colloid nanocrystal cluster (MCNC) as the core and COFs as the shell, while COFs were prepared by Schiff base condensation of 2,5-divinylterephthalaldehyde (Dva) and 1,3,5-tris(4-aminophenyl)benzene (Tab). Next, GSH was adorned onto the COF shell by thiol-ene “click” reaction to prepare MCNC@COF@GSH platform (Figure 17). The MCNC@

COF@GSH microspheres exhibited excellent performance for endogenous *N*-linked glycopeptide enrichment in human saliva with demonstrable reusability, high selectivity, and low detection limit.¹²⁵

The COF-300-AR with good reusability, light-control, high stability, and catalytic oxidation capacity has been fabricated in several steps. First, COF-300 was formed through the condensation of terephthalaldehyde (PDA) and tetrakis(4-aminophenyl)methane (TAPM). Consequently, terephthalic acid (TPA) was added to the ensuing COF-300 and reduced in the presence of NaBH₄ to generate COF-300-AR. The COF-300-AR showed oxidase-mimicking activity upon visible light irradiation with $\lambda = 400$ nm; detection of GSH levels in HL-60 cells (cell lysate) could be achieved with excellent sensitivity and high selectivity.¹²⁶

Li and co-workers devised an electrochemical sensing platform for the determination of prostate-specific antigen (PSA) using black phosphorene (BPene) as a substrate material and magnetic COFs as the nanoprobe. The fabricated immunosensor exhibited good stability and fine specificity with a low detection limit of 30 fg mL⁻¹ in the linear range of 0.0001 ng mL⁻¹ to 10 ng mL⁻¹.¹²⁷

TpTTA-COF was synthesized via the condensation of Tp with TTA under solvothermal conditions. The COF-based platform was demonstrated for sensing adenosine 5'-triphosphate and DNA.¹²⁸

2D imine-linked COF nanosheets have been explored as a fluorescence-sensing platform for the detection of DNA with high selectivity and excellent sensitivity. Ultrathin 2D COF nanosheets were fabricated by the condensation of tris(4-aminophenyl)amine (TAPA) with tris(4-formylphenyl)amine (TFPA), which was then exfoliated to obtain COF nanosheets via one-step solvent-assisted liquid sonication.¹²⁹ The fabricated biosensor exhibited a linear relationship between increased fluorescence intensity and the concentration of the target DNA, with a detection limit of 20×10^{-12} M. This is comparable with most 2D nanosheet-based fluorescence DNA sensors such as graphene oxide (detection limit of 2×10^{-9} M), carbon nitride (81×10^{-12} M),¹³⁰ MoS₂ (0.5×10^{-9} M),¹³¹ WS₂ (60×10^{-12} M),¹³² TaS₂ (50×10^{-12} M),¹³³ and MOF (20×10^{-12} M).¹³⁴ Furthermore, COFs have been reported for ultrasensitive detection of miRNAs.¹³⁵ The representative COF-based biosensing systems are summarized in Table 3.

9. ENZYME IMMOBILIZATION

Despite the fact that enzyme immobilization has high specificity and catalytic efficiency, the natural enzyme activity is difficult to maintain and the delivery is often complicated. Nanomaterial-based artificial enzymes, named nanozymes, have garnered great interest due to their facile production, long storage time, low cost, high stability, and greater resistance to biodegradation.¹³⁶ But the fabrication of nanozymes with high enantioselectivity and activity is still a great challenge. In this content, chiral COF nanozymes with substrate-binding sites and highly ordered active centers have been reported. Initially, Fe-COF was constructed by the Schiff-base reaction between iron 5,10,15,20-tetrakis(40-tetraphenylamino) porphyrin and terephthalaldehyde. Then the ensued Fe-COF was modified via postsynthetic modification route by adding L-histidine (L-His) as the chiral binding site to create L-Hisx@Fe-COF, which displayed 21.7-times higher activity compared to the natural enzyme (horse radish peroxidase). Furthermore, based on the chirality of the His unit, the COF nanozymes in the oxidation of dopa have shown high enantioselectivity.¹³⁷

In another work, MOFs were applied as sacrificial templates to fabricate hollow COF capsules for enzyme encapsulation. This effective, scalable, and facile method achieved high-performance COF bioreactors that could maintain enzyme conformational freedom, offered protective effect against the external environment, stabilized the enzyme, and enhanced mass transfer thus boosting the enzymatic activities. Compared to traditional porous materials such as SBA-15, the encapsulated enzymes in COF capsules showed excellent reusability. Furthermore, this platform exhibited high tunability and versatility; assorted COF shells, various sacrificial MOF templates, and different enzymes could be used.¹³⁸

In another research, ultrafine platinum NPs confined in a COF (Pt/COF) have been developed, which showed good catalytic activities; Pt NPs were grown *in situ* and confined in the COF with a narrow size distribution and the size as small as 2.44 nm. This Pt/COF catalyst exhibited high affinity and both superior oxidase-like and peroxidase-like activity toward the peroxidase (TMB) substrate.¹³⁹

These results have revealed that the COF nanozyme opens up a new avenue to overcome the present drawbacks of enzymatic immobilization in porous materials.

10. ANTICANCER ACTIVITIES

Cancer is abnormal cell growth having the potential to invade or spread to other parts of the body with inclusionary criteria around the globe that annually kill millions of people by cancer disease.^{140,141} There are several different factors, including smoking, tobacco, polluted air, chemicals, food, radiation, certain metals, infectious agents, genetic mutations, body immune system, and hormonal disorders, that can cause cancer.¹⁴² Therefore, the fabrication of new materials with anticancer activity is crucial in cancer therapy. In this context, Bhaumik et al. created a 2D TrzCOF structure by polycondensation of 2,4,6-tris(4-aminophenyl)-1,3,5-triazine (TAPT) with 1,3,5-tri(4-formylbiphenyl) benzene [Ph₇(CHO)₃, TFBPB] under solvothermal synthesis protocol. *In vitro* studies were performed on this 2D hexagonal TrzCOF that displayed anticancer activity for the colorectal carcinoma HCT-116 cells.¹⁴³ There is a need for evaluation of the validity of TrzCOF *in vivo* for clinical trials.

11. CONCLUSION AND OUTLOOK

As a new type of porous material, COFs possess unique characteristics and several advantages such as highly tunable porosity, ordered channels, biocompatibility, multifunctionality, large specific surface area, optional building blocks, and predictable and stable structure. These properties have endowed COF materials with superior potential applications in biomedical systems. Herein, we have discussed and reviewed the recent progress and achievements of 2D and 3D COF-based materials including their synthesis and functionalization and especially biomedical applications in the delivery of drugs and genes, bioimaging, biosensing, PDT, PTT, and combination therapy. Furthermore, the developmental prospects and challenges of COFs for biomedical appliances are deliberated with examples of COF-based platforms in both *in vitro* and *in vivo* models. Finally, recent efforts to develop various types of COFs-based platforms are highlighted that can overcome their traditional shortcomings. Furthermore, the high π -electron density of COFs along with the large surface area renders them a good candidate for bioimaging and biosensing. Nevertheless, despite these advantages, COFs suffer from several drawbacks such as poor physiological stability and scalability that will need detailed analysis and exploration. COF as an advantageous platform could be applied in newer approaches to cancer therapy, from novel drugs, biological agent, and drug delivery system to gene targeting, gene therapy, and the possibility of targeting cancer stem cells. Stimuli-responsive based COFs such as ROS-responsive, thermoresponsive, among others need more attention. So far, only two reports have demonstrated the use of 2D and 3D COF-based material for gene delivery. Therefore, COF-based gene delivery requires additional studies for realizing their full potential. Furthermore, there has been a clear lapse in extensive *in vivo* studies using 2D and 3D COF-based material, which could have paved the way to clinical trials. In view of the deployment of MOFs for biomedicine application, integration of COFs and MOFs-based strategies could be explored in the near future. Despite some general similarity such as biocompatibility and low cytotoxicity, there are differences between 2D and 3D COF in terms of shape, pore size and

porosity, and surface area, among others. These differences in characteristic offer different results in their application in the biomedical field such as drug and gene delivery, but to the best of our knowledge, there is not any research that has compared 2D and 3D COF in biomedical application. Consequently, in the future explorations, this comparison could be evaluated by researchers in this burgeoning field.

AUTHOR INFORMATION

Corresponding Authors

Hossein Yazdani – Department of Organic Chemistry, Shahid Beheshti University G.C., Tehran 1983963113, Iran; orcid.org/0000-0003-4317-8848; Email: hyazdani21@gmail.com

Rajender S. Varma – Regional Centre of Advanced Technologies and Materials, Czech Advanced Technology and Research Institute Palacký University in Olomouc, 783 71 Olomouc, Czech Republic; orcid.org/0000-0001-9731-6228; Email: varma.rajender@epa.gov

Author

Mohammad-Ali Shahbazi – Department of Biomedical Engineering, University of Groningen, University Medical Center Groningen, 9713 AV Groningen, The Netherlands; Zanjan Pharmaceutical Nanotechnology Research Center (ZPNRC), Zanjan University of Medical Sciences, 45139-46184 Zanjan, Iran; orcid.org/0000-0002-4860-3017

Complete contact information is available at: <https://pubs.acs.org/10.1021/acsabm.1c01015>

Author Contributions

H.Y. conceived, wrote, edited, revised, and guided this work. M.-A.S. edited and revised the manuscript. R.S.V. edited, revised, and guided the work.

Notes

The authors declare no competing financial interest.

REFERENCES

- (1) Cote, A. P.; Benin, A. I.; Ockwig, N. W.; O’Keeffe, M.; Matzger, A. J.; Yaghi, O. M. Porous, crystalline, covalent organic frameworks. *Science* **2005**, *310* (5751), 1166–1170.
- (2) Fang, Q.; Wang, J.; Gu, S.; Kaspar, R. B.; Zhuang, Z.; Zheng, J.; Guo, H.; Qiu, S.; Yan, Y. 3D Porous Crystalline Polyimide Covalent Organic Frameworks for Drug Delivery. *J. Am. Chem. Soc.* **2015**, *137* (26), 8352–8355.
- (3) Liu, Y.; Ma, Y.; Zhao, Y.; Sun, X.; Gándara, F.; Furukawa, H.; Liu, Z.; Zhu, H.; Zhu, C.; Suenaga, K.; Oleynikov, P.; Alshammari, A. S.; Zhang, X.; Terasaki, O.; Yaghi, O. M. Weaving of organic threads into a crystalline covalent organic framework. *Science* **2016**, *351* (6271), 365–369.
- (4) Kandambeth, S.; Venkatesh, V.; Shinde, D. B.; Kumari, S.; Halder, A.; Verma, S.; Banerjee, R. Self-templated chemically stable hollow spherical covalent organic framework. *Nat. Commun.* **2015**, *6* (1), 6786.
- (5) Wan, S.; Guo, J.; Kim, J.; Ihee, H.; Jiang, D. A Belt-Shaped, Blue Luminescent, and Semiconducting Covalent Organic Framework. *Angew. Chem., Int. Ed.* **2008**, *47* (46), 8826–8830.
- (6) Rodríguez-San-Miguel, D.; Montoro, C.; Zamora, F. Covalent organic framework nanosheets: preparation, properties and applications. *Chem. Soc. Rev.* **2020**, *49* (49), 2291–2302.
- (7) Huang, W.; Jiang, Y.; Li, X.; Li, X.; Wang, J.; Wu, Q.; Liu, X. Solvothermal Synthesis of Microporous, Crystalline Covalent Organic Framework Nanofibers and Their Colorimetric Nanohybrid Structures. *ACS Appl. Mater. Interfaces* **2013**, *5* (18), 8845–8849.
- (8) Mohammed, A. K.; Usgaonkar, S.; Kanheerampokil, F.; Karak, S.; Halder, A.; Tharkar, M.; Addicoat, M.; Ajithkumar, T. G.; Banerjee, R. Connecting Microscopic Structures, Mesoscale Assemblies, and Macroscopic Architectures in 3D-Printed Hierarchical Porous Covalent Organic Framework Foams. *J. Am. Chem. Soc.* **2020**, *142* (18), 8252–8261.
- (9) Lin, S.; Diercks, C. S.; Zhang, Y.-B.; Kornienko, N.; Nichols, E. M.; Zhao, Y.; Paris, A. R.; Kim, D.; Yang, P.; Yaghi, O. M.; Chang, C. J. Covalent organic frameworks comprising cobalt porphyrins for catalytic CO₂ reduction in water. *Science* **2015**, *349* (6253), 1208–1213.
- (10) Uribe-Romo, F. J.; Doonan, C. J.; Furukawa, H.; Oisaki, K.; Yaghi, O. M. Crystalline Covalent Organic Frameworks with Hydrazone Linkages. *J. Am. Chem. Soc.* **2011**, *133* (30), 11478–11481.
- (11) Cui, W.-R.; Zhang, C.-R.; Jiang, W.; Li, F.-F.; Liang, R.-P.; Liu, J.; Qiu, J.-D. Regenerable and stable sp² carbon-conjugated covalent organic frameworks for selective detection and extraction of uranium. *Nat. Commun.* **2020**, *11* (1), 1–10.
- (12) Stewart, D.; Antypov, D.; Dyer, M. S.; Pitcher, M. J.; Katsoulidis, A. P.; Chater, P. A.; Blanc, F.; Rosseinsky, M. J. Stable and ordered amide frameworks synthesised under reversible conditions which facilitate error checking. *Nat. Commun.* **2017**, *8* (1), 1–10.
- (13) Hisaki, I.; Suzuki, Y.; Gomez, E.; Ji, Q.; Tohnai, N.; Nakamura, T.; Douhal, A. Acid responsive hydrogen-bonded organic frameworks. *J. Am. Chem. Soc.* **2019**, *141* (5), 2111–2121.
- (14) Guan, X.; Li, H.; Ma, Y.; Xue, M.; Fang, Q.; Yan, Y.; Valtchev, V.; Qiu, S. Chemically stable polyarylether-based covalent organic frameworks. *Nat. Chem.* **2019**, *11* (6), 587–594.
- (15) Du, Y.; Yang, H.; Whiteley, J. M.; Wan, S.; Jin, Y.; Lee, S.-H.; Zhang, W. Ionic Covalent Organic Frameworks with Spiroborate Linkage. *Angew. Chem., Int. Ed.* **2016**, *55* (5), 1737–1741.
- (16) Wei, P.-F.; Qi, M.-Z.; Wang, Z.-P.; Ding, S.-Y.; Yu, W.; Liu, Q.; Wang, L.-K.; Wang, H.-Z.; An, W.-K.; Wang, W. Benzoxazole-linked ultrastable covalent organic frameworks for photocatalysis. *J. Am. Chem. Soc.* **2018**, *140* (13), 4623–4631.
- (17) Li, T.; Yan, X.; Liu, Y.; Zhang, W.-D.; Fu, Q.-T.; Zhu, H.; Li, Z.; Gu, Z.-G. A 2D covalent organic framework involving strong intramolecular hydrogen bonds for advanced supercapacitors. *Polym. Chem.* **2020**, *11* (1), 47–52.
- (18) Patra, B. C.; Khilari, S.; Satyanarayana, L.; Pradhan, D.; Bhaumik, A. A new benzimidazole based covalent organic polymer having high energy storage capacity. *Chem. Commun.* **2016**, *52* (48), 7592–7595.
- (19) Li, X.-T.; Zou, J.; Wang, T.-H.; Ma, H.-C.; Chen, G.-J.; Dong, Y.-B. Construction of Covalent Organic Frameworks via Three-Component One-Pot Strecker and Povarov Reactions. *J. Am. Chem. Soc.* **2020**, *142* (14), 6521–6526.
- (20) Wang, P.-L.; Ding, S.-Y.; Zhang, Z.-C.; Wang, Z.-P.; Wang, W. Constructing Robust Covalent Organic Frameworks via Multi-component Reactions. *J. Am. Chem. Soc.* **2019**, *141* (45), 18004–18008.
- (21) Rao, M. R.; Fang, Y.; De Feyter, S.; Perepichka, D. F. Conjugated covalent organic frameworks via michael addition-elimination. *J. Am. Chem. Soc.* **2017**, *139* (6), 2421–2427.
- (22) Jiang, S.-Y.; Gan, S.-X.; Zhang, X.; Li, H.; Qi, Q.-Y.; Cui, F.-Z.; Lu, J.; Zhao, X. Amino-Linked Covalent Organic Frameworks through Condensation of Secondary Amine with Aldehyde. *J. Am. Chem. Soc.* **2019**, *141* (38), 14981–14986.
- (23) Cote, A. P.; El-Kaderi, H. M.; Furukawa, H.; Hunt, J. R.; Yaghi, O. M. Reticular synthesis of microporous and mesoporous 2D covalent organic frameworks. *J. Am. Chem. Soc.* **2007**, *129* (43), 12914–12915.
- (24) Kuhn, P.; Antonietti, M.; Thomas, A. Porous, Covalent Triazine-Based Frameworks Prepared by Ionothermal Synthesis. *Angew. Chem., Int. Ed.* **2008**, *47* (18), 3450–3453.
- (25) Beaudoin, D.; Maris, T.; Wuest, J. D. Constructing monocrystalline covalent organic networks by polymerization. *Nat. Chem.* **2013**, *5* (10), 830–834.
- (26) Jackson, K. T.; Reich, T. E.; El-Kaderi, H. M. Targeted synthesis of a porous borazine-linked covalent organic framework. *Chem. Commun.* **2012**, *48* (70), 8823–8825.

- (27) Geng, K.; He, T.; Liu, R.; Dalapati, S.; Tan, K. T.; Li, Z.; Tao, S.; Gong, Y.; Jiang, Q.; Jiang, D. Covalent Organic Frameworks: Design, Synthesis, and Functions. *Chem. Rev.* **2020**, *120* (16), 8814–8933.
- (28) Sharma, R. K.; Yadav, P.; Yadav, M.; Gupta, R.; Rana, P.; Srivastava, A.; Zbořil, R.; Varma, R. S.; Antonietti, M.; Gawande, M. B. Recent development of covalent organic frameworks (COFs): synthesis and catalytic (organic-electro-photo) applications. *Mater. Horiz.* **2020**, *7* (2), 411–454.
- (29) Lohse, M. S.; Bein, T. Covalent organic frameworks: structures, synthesis, and applications. *Adv. Funct. Mater.* **2018**, *28* (33), 1705553.
- (30) Kandambeth, S.; Dey, K.; Banerjee, R. Covalent Organic Frameworks: Chemistry beyond the Structure. *J. Am. Chem. Soc.* **2019**, *141* (5), 1807–1822.
- (31) Campbell, N. L.; Clowes, R.; Ritchie, L. K.; Cooper, A. I. Rapid Microwave Synthesis and Purification of Porous Covalent Organic Frameworks. *Chem. Mater.* **2009**, *21* (2), 204–206.
- (32) Ren, S.; Bojdys, M. J.; Dawson, R.; Laybourn, A.; Khimyak, Y. Z.; Adams, D. J.; Cooper, A. I. Porous, Fluorescent, Covalent Triazine-Based Frameworks Via Room-Temperature and Microwave-Assisted Synthesis. *Adv. Mater.* **2012**, *24* (17), 2357–2361.
- (33) Bojdys, M. J.; Jeromenok, J.; Thomas, A.; Antonietti, M. Rational Extension of the Family of Layered, Covalent, Triazine-Based Frameworks with Regular Porosity. *Adv. Mater.* **2010**, *22* (19), 2202–2205.
- (34) Biswal, B. P.; Chandra, S.; Kandambeth, S.; Lukose, B.; Heine, T.; Banerjee, R. Mechanochemical Synthesis of Chemically Stable Isoreticular Covalent Organic Frameworks. *J. Am. Chem. Soc.* **2013**, *135* (14), 5328–5331.
- (35) Dey, K.; Pal, M.; Rout, K. C.; Kunjattu H, S.; Das, A.; Mukherjee, R.; Kharul, U. K.; Banerjee, R. Selective Molecular Separation by Interfacially Crystallized Covalent Organic Framework Thin Films. *J. Am. Chem. Soc.* **2017**, *139* (37), 13083–13091.
- (36) Yang, S.-T.; Kim, J.; Cho, H.-Y.; Kim, S.; Ahn, W.-S. Facile synthesis of covalent organic frameworks COF-1 and COF-5 by sonochemical method. *RSC Adv.* **2012**, *2* (27), 10179–10181.
- (37) Kim, S.; Choi, H. C. Light-promoted synthesis of highly-conjugated crystalline covalent organic framework. *Commun. Chem.* **2019**, *2* (1), 1–8.
- (38) Zhang, M.; Chen, J.; Zhang, S.; Zhou, X.; He, L.; Sheridan, M. V.; Yuan, M.; Zhang, M.; Chen, L.; Dai, X.; Ma, F.; Wang, J.; Hu, J.; Wu, G.; Kong, X.; Zhou, R.; Albrecht-Schmitt, T. E.; Chai, Z.; Wang, S. Electron Beam Irradiation as a General Approach for the Rapid Synthesis of Covalent Organic Frameworks under Ambient Conditions. *J. Am. Chem. Soc.* **2020**, *142* (20), 9169–9174.
- (39) Dey, K.; Kunjattu H, S.; Chahande, A. M.; Banerjee, R. Nanoparticle Size-Fractionation through Self-Standing Porous Covalent Organic Framework Films. *Angew. Chem.* **2020**, *132*, 1177–1181.
- (40) Wang, Z.; Zhang, S.; Chen, Y.; Zhang, Z.; Ma, S. Covalent organic frameworks for separation applications. *Chem. Soc. Rev.* **2020**, *49* (3), 708–735.
- (41) Zhang, K.; Kirlikovali, K. O.; Varma, R. S.; Jin, Z.; Jang, H. W.; Farha, O. K.; Shokouhimehr, M. Covalent Organic Frameworks: Emerging Organic Solid Materials for Energy and Electrochemical Applications. *ACS Appl. Mater. Interfaces* **2020**, *12* (25), 27821–27852.
- (42) Zhu, H.; Lin, W.; Li, Q.; Hu, Y.; Guo, S.; Wang, C.; Yan, F. Bipyridinium-Based Ionic Covalent Triazine Frameworks for CO₂, SO₂, and NO Capture. *ACS Appl. Mater. Interfaces* **2020**, *12* (7), 8614–8621.
- (43) Dong, Y.-B.; Guan, Q.; Zhou, L.-L.; Li, W.-Y.; Li, Y.-A. Covalent Organic Frameworks (COFs) for Cancer Therapeutics. *Chem. - Eur. J.* **2020**, *26* (25), 1–10.
- (44) Scicluna, M. C.; Vella-Zarb, L. Evolution of Nanocarrier Drug-Delivery Systems and Recent Advancements in Covalent Organic Framework-Drug Systems. *ACS Appl. Nano Mater.* **2020**, *3* (4), 3097–3115.
- (45) Bhunia, S.; Deo, K. A.; Gaharwar, A. K. 2D Covalent Organic Frameworks for Biomedical Applications. *Adv. Funct. Mater.* **2020**, *30* (27), 2002046.
- (46) Esrafil, A.; Wagner, A.; Inamdar, S.; Acharya, A. P. Covalent Organic Frameworks for Biomedical Applications. *Adv. Healthcare Mater.* **2021**, *10* (6), 2002090.
- (47) Feng, L.; Qian, C.; Zhao, Y. Recent Advances in Covalent Organic Framework-Based Nanosystems for Bioimaging and Therapeutic Applications. *ACS Materials Lett.* **2020**, *2* (9), 1074–1092.
- (48) Bhattacharya, K.; Banerjee, S. L.; Das, S.; Samanta, S.; Mandal, M.; Singha, N. K. REDOX Responsive Fluorescence Active Glycopolymer Based Nanogel: A Potential Material for Targeted Anticancer Drug Delivery. *ACS Appl. Bio Mater.* **2019**, *2* (6), 2587–2599.
- (49) Sabourian, P.; Tavakolian, M.; Yazdani, H.; Frounchi, M.; van de Ven, T. G. M.; Maysinger, D.; Kakkar, A. Stimuli-responsive chitosan as an advantageous platform for efficient delivery of bioactive agents. *J. Controlled Release* **2020**, *317*, 216–231.
- (50) Oroojalian, F.; Beygi, M.; Baradaran, B.; Mokhtarzadeh, A.; Shahbazi, M.-A. Immune Cell Membrane-Coated Biomimetic Nanoparticles for Targeted Cancer Therapy. *Small* **2021**, *17* (12), 2006484.
- (51) Shahbazi, M.-A.; Faghfour, L.; Ferreira, M. P.; Figueiredo, P.; Maleki, H.; Sefat, F.; Hirvonen, J.; Santos, H. A. The versatile biomedical applications of bismuth-based nanoparticles and composites: therapeutic, diagnostic, biosensing, and regenerative properties. *Chem. Soc. Rev.* **2020**, *49* (4), 1253–1321.
- (52) Makvandi, P.; Baghbantarghadari, Z.; Zhou, W.; Zhang, Y.; Manchanda, R.; Agarwal, T.; Wu, A.; Maiti, T. K.; Varma, R. S.; Smith, B. R. Gum polysaccharide/nanometal hybrid biocomposites in cancer diagnosis and therapy. *Biotechnol. Adv.* **2021**, *48*, 107711.
- (53) Zhao, H.; Jin, Z.; Su, H.; Jing, X.; Sun, F.; Zhu, G. Targeted synthesis of a 2D ordered porous organic framework for drug release. *Chem. Commun.* **2011**, *47* (22), 6389–6391.
- (54) Horcajada, P.; Serre, C.; Vallet-Regi, M.; Sebban, M.; Taulelle, F.; Ferey, G. Metal-organic frameworks as efficient materials for drug delivery. *Angew. Chem., Int. Ed.* **2006**, *45* (36), 5974–5978.
- (55) Horcajada, P.; Serre, C.; Maurin, G.; Ramsahye, N. A.; Balas, F.; Vallet-Regi, M.; Sebban, M.; Taulelle, F.; Ferey, G. Flexible porous metal-organic frameworks for a controlled drug delivery. *J. Am. Chem. Soc.* **2008**, *130* (21), 6774–6780.
- (56) Bai, L.; Phua, S. Z. F.; Lim, W. Q.; Jana, A.; Luo, Z.; Tham, H. P.; Zhao, L.; Gao, Q.; Zhao, Y. Nanoscale covalent organic frameworks as smart carriers for drug delivery. *Chem. Commun.* **2016**, *52* (22), 4128–4131.
- (57) Vyas, V. S.; Vishwakarma, M.; Moudrakovski, I.; Haase, F.; Savasci, G.; Ochsenfeld, C.; Spatz, J. P.; Lotsch, B. V. Exploiting Noncovalent Interactions in an Imine-Based Covalent Organic Framework for Quercetin Delivery. *Adv. Mater.* **2016**, *28* (39), 8749–8754.
- (58) Mitra, S.; Sasmal, H. S.; Kundu, T.; Kandambeth, S.; Illath, K.; Díaz Díaz, D.; Banerjee, R. Targeted Drug Delivery in Covalent Organic Nanosheets (CONs) via Sequential Postsynthetic Modification. *J. Am. Chem. Soc.* **2017**, *139* (12), 4513–4520.
- (59) Zhang, G.; Li, X.; Liao, Q.; Liu, Y.; Xi, K.; Huang, W.; Jia, X. Water-dispersible PEG-curcumin/aminefunctionalized covalent organic framework nanocomposites as smart carriers for in vivo drug delivery. *Nat. Commun.* **2018**, *9* (1), 2785–2795.
- (60) Lotocki, V.; Yazdani, H.; Zhang, Q.; Gran, E. R.; Nyrko, A.; Maysinger, D.; Kakkar, A. Miktoarm Star Polymers with Environment-Selective ROS/GSH Responsive Locations: From Modular Synthesis to Tuned Drug Release through Micellar Partial Corona Shedding and/or Core Disassembly. *Macromol. Biosci.* **2021**, *21* (2), 2000305.
- (61) Karimzadeh, S.; Javanbakht, S.; Baradaran, B.; Shahbazi, M.-A.; Hashemzadei, M.; Mokhtarzadeh, A.; Santos, H. A. Synthesis and Therapeutic Potential of Stimuli-responsive Metal-Organic Frameworks. *Chem. Eng. J.* **2021**, *408*, 127233.
- (62) Delfi, M.; Sartorius, R.; Ashrafzadeh, M.; Sharifi, E.; Zhang, Y.; De Berardinis, P.; Zarrabi, A.; Varma, R. S.; Tay, F. R.; Smith, B. R.; et al. Self-assembled peptide and protein nanostructures for anti-cancer therapy: Targeted delivery, stimuli-responsive devices and immunotherapy. *Nano Today* **2021**, *38*, 101119.

- (63) Lushchak, V. I. Glutathione homeostasis and functions potential targets for medical interventions. *J. Amino Acids* **2012**, *2012*, 1–26.
- (64) Traverso, N.; Ricciarelli, R.; Nitti, M.; Marengo, B.; Furfaro, A. L.; Pronzato, M. A.; Marinari, U. M.; Domenicotti, C. Role of glutathione in cancer progression and chemoresistance. *Oxid. Med. Cell. Longevity* **2013**, *2013*, 1–10.
- (65) Quinn, J. F.; Whittaker, M. R.; Davis, T. P. Glutathione responsive polymers and their application in drug delivery systems. *Polym. Chem.* **2017**, *8* (1), 97–126.
- (66) Liu, S.; Yang, J.; Guo, R.; Deng, L.; Dong, A.; Zhang, J. Facile Fabrication of Redox-Responsive Covalent Organic Framework Nanocarriers for Efficiently Loading and Delivering Doxorubicin. *Macromol. Rapid Commun.* **2020**, *41* (4), 1900570–1900575.
- (67) Kocak, G.; Tuncer, C.; Bütün, V. pH-Responsive polymers. *Polym. Chem.* **2017**, *8* (1), 144–176.
- (68) Wang, B.; Liu, X.; Gong, P.; Ge, X.; Liu, Z.; You, J. Fluorescent COFs with a highly conjugated structure for visual drug loading and responsive release. *Chem. Commun.* **2020**, *56* (4), 519–522.
- (69) Liu, S.; Hu, C.; Liu, Y.; Zhao, X.; Pang, M.; Lin, J. One-Pot Synthesis of DOX@Covalent Organic Framework with Enhanced Chemotherapeutic Efficacy. *Chem. - Eur. J.* **2019**, *25* (17), 4315–4319.
- (70) Akyuz, L. An imine based COF as a smart carrier for targeted drug delivery: From synthesis to computational studies. *Microporous Mesoporous Mater.* **2020**, *294*, 109850.
- (71) Mintzer, M. A.; Simanek, E. E. Nonviral vectors for gene delivery. *Chem. Rev.* **2009**, *109* (2), 259–302.
- (72) Zhou, Z.; Liu, X.; Zhu, D.; Wang, Y.; Zhang, Z.; Zhou, X.; Qiu, N.; Chen, X.; Shen, Y. Nonviral cancer gene therapy: Delivery cascade and vector nanoproperty integration. *Adv. Drug Delivery Rev.* **2017**, *115*, 115–154.
- (73) Wang, H.-X.; Li, M.; Lee, C. M.; Chakraborty, S.; Kim, H.-W.; Bao, G.; Leong, K. W. CRISPR/Cas9-based genome editing for disease modeling and therapy: challenges and opportunities for nonviral delivery. *Chem. Rev.* **2017**, *117* (15), 9874–9906.
- (74) Buck, J.; Grossen, P.; Cullis, P. R.; Huwyler, J. r.; Witzigmann, D. Lipid-based DNA therapeutics: hallmarks of non-viral gene delivery. *ACS Nano* **2019**, *13* (4), 3754–3782.
- (75) Xu, X.; Hou, S.; Wattanatorn, N.; Wang, F.; Yang, Q.; Zhao, C.; Yu, X.; Tseng, H.-R.; Jonas, S. J.; Weiss, P. S. Precision-guided nanospears for targeted and high-throughput intracellular gene delivery. *ACS Nano* **2018**, *12* (5), 4503–4511.
- (76) Cao, Y.; Zhang, J.; Wang, L.; Cen, M.; Peng, W.; Li, Y.; Zhang, F.; Tan, J.; Fan, X. Dual-Functionalized Covalent Triazine Framework Nanosheets as Hierarchical Nonviral Vectors for Intracellular Gene Delivery. *ACS Appl. Nano Mater.* **2021**, *4* (5), 4948–4955.
- (77) Hao, K.; Guo, Z.; Lin, L.; Sun, P.; Li, Y.; Tian, H.; Chen, X. Covalent organic framework nanoparticles for anti-tumor gene therapy. *Sci. China: Chem.* **2021**, *64* (7), 1–7.
- (78) Lee, H. P.; Gaharwar, A. K. Light-Responsive Inorganic Biomaterials for Biomedical Applications. *Adv. Sci.* **2020**, *7* (17), 2000863.
- (79) Sun, Q.; Bi, H.; Wang, Z.; Li, C.; Wang, C.; Xu, J.; Yang, D.; He, F.; Gai, S.; Yang, P. O₂-Generating Metal-Organic Framework-Based Hydrophobic Photosensitizer Delivery System for Enhanced Photodynamic Therapy. *ACS Appl. Mater. Interfaces* **2019**, *11* (40), 36347–36358.
- (80) Chen, L.; Yang, Y.; Zhang, P.; Wang, S.; Xu, J.-F.; Zhang, X. Degradable Supramolecular Photodynamic Polymer Materials for Biofilm Elimination. *ACS Appl. Bio Mater.* **2019**, *2* (7), 2920–2926.
- (81) Tian, J.; Xiao, C.; Huang, B.; Jiang, X.; Cao, H.; Liu, F.; Zhang, W. Combating Multidrug Resistance through an NIR-Triggered Cyanine-Containing Amphiphilic Block Copolymer. *ACS Appl. Bio Mater.* **2019**, *2* (5), 1862–1874.
- (82) Ormond, A.; Freeman, H. Dye Sensitizers for Photodynamic Therapy. *Materials* **2013**, *6* (3), 817–840.
- (83) Lin, Q.; Bao, C.; Yang, Y.; Liang, Q.; Zhang, D.; Cheng, S.; Zhu, L. Highly Discriminating Photorelease of Anticancer Drugs Based on Hypoxia Activatable Phototrigger Conjugated Chitosan Nanoparticles. *Adv. Mater.* **2013**, *25* (14), 1981–1986.
- (84) Xia, G.; Wang, H. Squaraine dyes: The hierarchical synthesis and its application in optical detection. *J. Photochem. Photobiol., C* **2017**, *31*, 84–113.
- (85) Amaro, M.; Filipe, H. A.; Ramalho, J. P.; Hof, M.; Loura, L. M. Fluorescence of nitrobenzoxadiazole (NBD)-labeled lipids in model membranes is connected not to lipid mobility but to probe location. *Phys. Chem. Chem. Phys.* **2016**, *18* (10), 7042–7054.
- (86) Whitaker, J. E.; Haugland, R. P.; Moore, P. L.; Hewitt, P. C.; Reese, M.; Haugland, R. P. Cascade Blue derivatives: water soluble, reactive, blue emission dyes evaluated as fluorescent labels and tracers. *Anal. Biochem.* **1991**, *198* (1), 119–130.
- (87) Miranda, C.; Bettencourt, S.; Pozdniakova, T.; Pereira, J.; Sampaio, P.; Franco-Duarte, R.; Pais, C. Modified high-throughput Nile red fluorescence assay for the rapid screening of oleaginous yeasts using acetic acid as carbon source. *BMC Microbiol.* **2020**, *20* (1), 1–11.
- (88) Lu, J.-Y.; Zhang, P.-L.; Chen, Q.-Y. A Nano-BODIPY Encapsulated Zeolitic Imidazolate Framework As Photoresponsive Integrating Antibacterial Agent. *ACS Appl. Bio Mater.* **2020**, *3* (1), 458–465.
- (89) Wu, L.; Sedgwick, A. C.; Sun, X.; Bull, S. D.; He, X.-P.; James, T. D. Reaction-based fluorescent probes for the detection and imaging of reactive oxygen, nitrogen, and sulfur species. *Acc. Chem. Res.* **2019**, *52* (9), 2582–2597.
- (90) Wu, D.; Chen, L.; Xu, Q.; Chen, X.; Yoon, J. Design principles, sensing mechanisms, and applications of highly specific fluorescent probes for HOCl/OCl⁻. *Acc. Chem. Res.* **2019**, *52* (8), 2158–2168.
- (91) Que, Y.; Liu, Y.; Tan, W.; Feng, C.; Shi, P.; Li, Y.; Huang, X. Enhancing Photodynamic Therapy Efficacy by Using Fluorinated Nanoplatform. *ACS Macro Lett.* **2016**, *5* (2), 168–173.
- (92) Pan, D.; Liang, P.; Zhong, X.; Wang, D.; Cao, H.; Wang, W.; He, W.; Yang, Z.; Dong, X. Self-Assembled Porphyrin-Based Nanoparticles with Enhanced Near-Infrared Absorbance for Fluorescence Imaging and Cancer Photodynamic Therapy. *ACS Appl. Bio Mater.* **2019**, *2* (3), 999–1005.
- (93) Dong, Y.-B.; Guan, Q.; Zhou, L.-L.; Li, W.-Y.; Li, Y.-A. Covalent Organic Frameworks (COFs) for Cancer Therapeutics. *Chem. - Eur. J.* **2020**, *26*, 1–10.
- (94) Chen, J.; Zhu, Y.; Kaskel, S. Porphyrin-Based Metal-Organic Frameworks for Biomedical Applications. *Angew. Chem., Int. Ed.* **2021**, *60* (10), 5010–5035.
- (95) Hynek, J.; Zelenka, J.; Rathouský, J. i.; Kubát, P.; Ruml, T. s.; Demel, J.; Lang, K. Designing porphyrinic covalent organic frameworks for the photodynamic inactivation of bacteria. *ACS Appl. Mater. Interfaces* **2018**, *10* (10), 8527–8535.
- (96) Zhang, Y.; Zhang, L.; Wang, Z.; Wang, F.; Kang, L.; Cao, F.; Dong, K.; Ren, J.; Qu, X. Renal-clearable ultrasmall covalent organic framework nanodots as photodynamic agents for effective cancer therapy. *Biomaterials* **2019**, *223*, 119462–119471.
- (97) Wang, H.; Wang, Z.; Li, Y.; Xu, T.; Zhang, Q.; Yang, M.; Wang, P.; Gu, Y. A Novel Theranostic Nanoprobe for In Vivo Singlet Oxygen Detection and Real-Time Dose-Effect Relationship Monitoring in Photodynamic Therapy. *Small* **2019**, *15* (39), 1902185.
- (98) Yuan, Y.; Zhang, C.-J.; Kwok, R. T. K.; Xu, S.; Zhang, R.; Wu, J.; Tang, B. Z.; Liu, B. Light-Up Probe for Targeted and Activatable Photodynamic Therapy with Real-Time In Situ Reporting of Sensitizer Activation and Therapeutic Responses. *Adv. Funct. Mater.* **2015**, *25* (42), 6586–6595.
- (99) Wang, P.; Zhou, F.; Guan, K.; Wang, Y.; Fu, X.; Yang, Y.; Yin, X.; Song, G.; Zhang, X.; Tan, W. In vivo therapeutic response monitoring by a selfreporting upconverting covalent organic framework nanoplat-form. *Chem. Sci.* **2020**, *11* (5), 1299–1306.
- (100) Wang, S.-B.; Chen, Z.-X.; Gao, F.; Zhang, C.; Zou, M.-Z.; Ye, J.-J.; Zeng, X.; Zhang, X.-Z. Remodeling extracellular matrix based on functional covalent organic framework to enhance tumor photodynamic therapy. *Biomaterials* **2020**, *234*, 119772–119781.
- (101) Zhang, L.; Wang, S.; Zhou, Y.; Wang, C.; Zhang, X. Z.; Deng, H. Covalent Organic Frameworks as Favorable Constructs for Photodynamic Therapy. *Angew. Chem.* **2019**, *131* (40), 14351–14356.

- (102) Zhao, Y.; Dai, W.; Peng, Y.; Niu, Z.; Sun, Q.; Shan, C.; Yang, H.; Verma, G.; Wojtas, L.; Yuan, D.; Zhang, Z.; Dong, H.; Zhang, X.; Zhang, B.; Feng, Y.; Ma, S. A Corrole-Based Covalent Organic Framework Featuring Desymmetric Topology. *Angew. Chem., Int. Ed.* **2020**, *59* (11), 4354–4359.
- (103) Du, Y.; Calabro, D.; Wooler, B.; Kortunov, P.; Li, Q.; Cundy, S.; Mao, K. One step facile synthesis of amine-functionalized COF-1 with enhanced hydrostability. *Chem. Mater.* **2015**, *27* (5), 1445–1447.
- (104) Tong, X.; Gan, S.; Wu, J.; Hu, Y.; Yuan, A. A nano-photosensitizer based on covalent organic framework nanosheets with high loading and therapeutic efficacy. *Nanoscale* **2020**, *12* (13), 7376–7382.
- (105) Guan, Q.; Fu, D.-D.; Li, Y.-A.; Kong, X.-M.; Wei, Z.-Y.; Li, W.-Y.; Zhang, S.-J.; Dong, Y.-B. BODIPY-decorated nanoscale covalent organic frameworks for photodynamic therapy. *iScience* **2019**, *14*, 180–198.
- (106) Ouyang, B.; Liu, F.; Ruan, S.; Liu, Y.; Guo, H.; Cai, Z.; Yu, X.; Pang, Z.; Shen, S. Localized Free Radicals Burst Triggered by NIR-II Light for Augmented Low-Temperature Photothermal Therapy. *ACS Appl. Mater. Interfaces* **2019**, *11* (42), 38555–38567.
- (107) Shi, Y.; Liu, S.; Zhang, Z.; Liu, Y.; Pang, M. Template-free synthesis and metalation of hierarchical covalent organic framework spheres for photothermal therapy. *Chem. Commun.* **2019**, *55* (95), 14315–14318.
- (108) Tan, J.; Namuangruk, S.; Kong, W.; Kungwan, N.; Guo, J.; Wang, C. Manipulation of amorphous-to-crystalline transformation: Towards the construction of covalent organic framework hybrid microspheres with NIR photothermal conversion ability. *Angew. Chem., Int. Ed.* **2016**, *55* (45), 13979–13984.
- (109) Li, B.; Lv, Y.-K.; Wang, Z.-D.; Peng, P.; Zang, S.-Q. Edge confined covalent organic framework with efficient biocompatibility and photothermic conversion. *Nano Today* **2021**, *37*, 101101.
- (110) Liu, S.; Liu, Y.; Hu, C.; Zhao, X.; Pang, M.; et al. Boosting the antitumor efficacy over a nanoscale porphyrin-based covalent organic polymer via synergistic photodynamic and photothermal therapy. *Chem. Commun.* **2019**, *55* (44), 6269–6272.
- (111) Wan, X.; Zhang, H.; Pan, W.; Li, N.; Tang, B. An Enzyme Nanopocket Based on Covalent Organic Frameworks for Long-Termed Starvation Therapy and Enhanced Photodynamic Therapy of Cancer. *Chem. Commun.* **2021**, *57* (44), 5402–5405.
- (112) Gan, S.; Tong, X.; Zhang, Y.; Wu, J.; Hu, Y.; Yuan, A. Covalent Organic Framework-Supported Molecularly Dispersed Near-Infrared Dyes Boost Immunogenic Phototherapy against Tumors. *Adv. Funct. Mater.* **2019**, *29* (46), 1902757–1902770.
- (113) Calik, M.; Auras, F.; Salonen, L. M.; Bader, K.; Grill, I.; Handloser, M.; Medina, D. D.; Dogru, M.; Löbermann, F.; Trauner, D.; Hartschuh, A.; Bein, T. Extraction of Photogenerated Electrons and Holes from a Covalent Organic Framework Integrated Heterojunction. *J. Am. Chem. Soc.* **2014**, *136* (51), 17802–17807.
- (114) Wang, K.; Zhang, Z.; Lin, L.; Chen, J.; Hao, K.; Tian, H.; Chen, X. Covalent Organic Nanosheets Integrated Heterojunction with Two Strategies To Overcome Hypoxic-Tumor Photodynamic Therapy. *Chem. Mater.* **2019**, *31* (9), 3313–3323.
- (115) Hu, C.; Zhang, Z.; Liu, S.; Liu, X.; Pang, M. Monodispersed CuSe Sensitized Covalent Organic Framework Photosensitizer with an Enhanced Photodynamic and Photothermal Effect for Cancer Therapy. *ACS Appl. Mater. Interfaces* **2019**, *11* (26), 23072–23082.
- (116) Guan, Q.; Zhou, L.-L.; Li, Y.-A.; Li, W.-Y.; Wang, S.; Song, C.; Dong, Y.-B. Nanoscale Covalent Organic Framework for Combinatorial Antitumor Photodynamic and Photothermal Therapy. *ACS Nano* **2019**, *13* (11), 13304–13316.
- (117) Wang, D.; Zhang, Z.; Lin, L.; Liu, F.; Wang, Y.; Guo, Z.; Li, Y.; Tian, H.; Chen, X. Porphyrin-based covalent organic framework nanoparticles for photoacoustic imaging-guided photodynamic and photothermal combination cancer therapy. *Biomaterials* **2019**, *223*, 119459.
- (118) Wang, K.; Zhang, Z.; Lin, L.; Hao, K.; Chen, J.; Tian, H.; Chen, X. Cyanine-Assisted Exfoliation of Covalent Organic Frameworks in Nanocomposites for Highly Efficient Chemo-Photothermal Tumor Therapy. *ACS Appl. Mater. Interfaces* **2019**, *11* (43), 39503–39512.
- (119) Cheng, H.-B.; Li, Y.; Tang, B. Z.; Yoon, J. Assembly strategies of organic-based imaging agents for fluorescence and photoacoustic bioimaging applications. *Chem. Soc. Rev.* **2020**, *49* (1), 21–31.
- (120) Sharma, P.; Brown, S.; Walter, G.; Santra, S.; Moudgil, B. Nanoparticles for bioimaging. *Adv. Colloid Interface Sci.* **2006**, *123–126*, 471–485.
- (121) Das, G.; Benyettou, F.; Sharama, S. K.; Prakasam, T.; Gándara, F.; Victor, A.; Saleh, N. i.; Pasricha, R.; Jagannathan, R.; Olson, M. A.; et al. Covalent organic nanosheets for bioimaging. *Chem. Sci.* **2018**, *9* (44), 8382–8387.
- (122) Wang, P.; Zhou, F.; Zhang, C.; Yin, S.-Y.; Teng, L.; Chen, L.; Hu, X.-X.; Liu, H.-W.; Yin, X.; Zhang, X.-B. Ultrathin two-dimensional covalent organic framework nanoprobe for interference-resistant two-photon fluorescence bioimaging. *Chem. Sci.* **2018**, *9* (44), 8402–8408.
- (123) Zeng, J. Y.; Wang, X. S.; Xie, B. R.; Li, M. J.; Zhang, X. Z. Covalent Organic Framework for Improving Near-Infrared Light Induced Fluorescence Imaging through Two-Photon Induction. *Angew. Chem.* **2020**, *132* (25), 10173–10180.
- (124) Zhang, X.; Li, G.; Wu, D.; Zhang, B.; Hu, N.; Wang, H.; Liu, J.; Wu, Y. Recent advances in the construction of functionalized covalent organic frameworks and their applications to sensing. *Biosens. Bioelectron.* **2019**, *145*, 111699–111717.
- (125) Luo, B.; He, J.; Li, Z.; Lan, F.; Wu, Y. Glutathione-Functionalized Magnetic Covalent Organic Framework Microspheres with Size Exclusion for Endogenous Glycopeptide Recognition in Human Saliva. *ACS Appl. Mater. Interfaces* **2019**, *11* (50), 47218–47226.
- (126) Jin, P.; Niu, X.; Zhang, F.; Dong, K.; Dai, H.; Zhang, H.; Wang, W.; Chen, H.; Chen, X. Stable and Reusable Light-responsive Reduced Covalent Organic Framework (COF-300-AR) as Oxidase-mimicking Catalyst for GSH Detection in Cell Lysate. *ACS Appl. Mater. Interfaces* **2020**, *12* (18), 20414–20422.
- (127) Liang, H.; Xu, H.; Zhao, Y.; Zheng, J.; Zhao, H.; Li, G.; Li, C.-P. Ultrasensitive electrochemical sensor for prostate specific antigen detection with a phosphorene platform and magnetic covalent organic framework signal amplifier. *Biosens. Bioelectron.* **2019**, *144*, 111691.
- (128) Li, W.; Yang, C.-X.; Yan, X.-P. A versatile covalent organic framework-based platform for sensing biomolecules. *Chem. Commun.* **2017**, *53* (83), 11469–11471.
- (129) Peng, Y.; Huang, Y.; Zhu, Y.; Chen, B.; Wang, L.; Lai, Z.; Zhang, Z.; Zhao, M.; Tan, C.; Yang, N.; et al. Ultrathin two-dimensional covalent organic framework nanosheets: preparation and application in highly sensitive and selective DNA detection. *J. Am. Chem. Soc.* **2017**, *139* (25), 8698–8704.
- (130) Wang, Q.; Wang, W.; Lei, J.; Xu, N.; Gao, F.; Ju, H. Fluorescence quenching of carbon nitride nanosheet through its interaction with DNA for versatile fluorescence sensing. *Anal. Chem.* **2013**, *85* (24), 12182–12188.
- (131) Zhu, C.; Zeng, Z.; Li, H.; Li, F.; Fan, C.; Zhang, H. Single-layer MoS₂-based nanoprobe for homogeneous detection of biomolecules. *J. Am. Chem. Soc.* **2013**, *135* (16), 5998–6001.
- (132) Yuan, Y.; Li, R.; Liu, Z. Establishing water-soluble layered WS₂ nanosheet as a platform for biosensing. *Anal. Chem.* **2014**, *86* (7), 3610–3615.
- (133) Zhang, Y.; Zheng, B.; Zhu, C.; Zhang, X.; Tan, C.; Li, H.; Chen, B.; Yang, J.; Chen, J.; Huang, Y.; et al. Single-layer transition metal dichalcogenide nanosheet-based nanosensors for rapid, sensitive, and multiplexed detection of DNA. *Adv. Mater.* **2015**, *27* (5), 935–939.
- (134) Zhao, M.; Wang, Y.; Ma, Q.; Huang, Y.; Zhang, X.; Ping, J.; Zhang, Z.; Lu, Q.; Yu, Y.; Xu, H.; et al. Ultrathin 2D metal-organic framework nanosheets. *Adv. Mater.* **2015**, *27* (45), 7372–7378.
- (135) Cao, Z.; Duan, F.; Huang, X.; Liu, Y.; Zhou, N.; Xia, L.; Zhang, Z.; Du, M. A multiple aptasensor for ultrasensitive detection of miRNAs by using covalent-organic framework nanowire as platform and shell-encoded gold nanoparticles as signal labels. *Anal. Chim. Acta* **2019**, *1082*, 176–185.

(136) Jiang, D.; Ni, D.; Rosenkrans, Z. T.; Huang, P.; Yan, X.; Cai, W. Nanozyme: new horizons for responsive biomedical applications. *Chem. Soc. Rev.* **2019**, *48* (14), 3683–3704.

(137) Zhou, Y.; Wei, Y.; Ren, J.; Qu, X. A chiral covalent organic framework (COF) nanozyme with ultrahigh enzymatic activity. *Mater. Horiz.* **2020**, *7* (12), 3291–3297.

(138) Li, M.; Qiao, S.; Zheng, Y.; Andaloussi, Y. H.; Li, X.; Zhang, Z.; Li, A.; Cheng, P.; Ma, S.; Chen, Y. Fabricating Covalent Organic Framework Capsules with Commodious Microenvironment for Enzymes. *J. Am. Chem. Soc.* **2020**, *142* (14), 6675–6681.

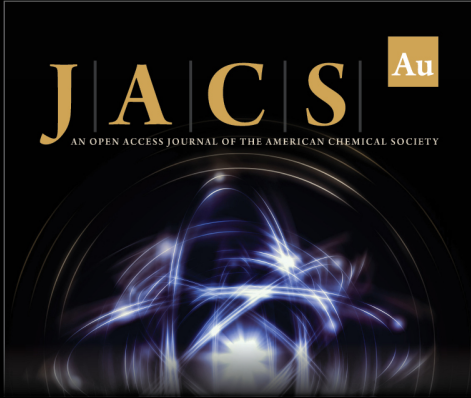
(139) Zhang, L.; Han, C.; Zhang, P.; Fu, W.; Nie, Y.; Wang, Y. Ultrafine platinum nanoparticles confined in a covalent organic framework for enhanced enzyme-mimetic and electrocatalytic performances. *Nanoscale* **2021**, *13* (44), 18665–18676.

(140) Castora, F. J. Mitochondrial function and abnormalities implicated in the pathogenesis of ASD. *Prog. Neuro-Psychopharmacol. Biol. Psychiatry* **2019**, *92*, 83–108.

(141) Yazdani, H.; Kaul, E.; Bazgir, A.; Maysinger, D.; Kakkar, A. Telodendrimer-Based Macromolecular Drug Design using 1,3-Dipolar Cycloaddition for Applications in Biology. *Molecules* **2020**, *25* (4), 857–868.


(142) Iqbal, J.; Abbasi, B. A.; Mahmood, T.; Kanwal, S.; Ali, B.; Shah, S. A.; Khalil, A. T. Plant-derived anticancer agents: A green anticancer approach. *Asian Pac. J. Trop. Biomed.* **2017**, *7* (12), 1129–1150.


(143) Kanti Das, S.; Mishra, S.; Manna, K.; Kayal, U.; Mahapatra, S.; Das Saha, K.; Dalapati, S.; Das, G. P.; Mostafa, A. A.; Bhaumik, A. A new triazine based π -conjugated mesoporous 2D covalent organic framework: its in vitro anticancer activities. *Chem. Commun.* **2018**, *54* (81), 11475–11478.



JACS Au
AN OPEN ACCESS JOURNAL OF THE AMERICAN CHEMICAL SOCIETY

Editor-in-Chief
Prof. Christopher W. Jones
Georgia Institute of Technology, USA

Open for Submissions 

pubs.acs.org/jacsau  ACS Publications
Most Trusted. Most Cited. Most Read.